bioRxiv preprint doi: https://doi.org/10.1101/795617; this version posted October 9, 2019. The copyright holder for this preprint (which was not certified by peer review) is the author/funder. All rights reserved. No reuse allowed without permission.

Title: *Salmonella* Enhances Osteogenic Differentiation in Adipose-Derived Mesenchymal Stem Cells

Running header: *Salmonella* alters MSC differentiation trajectory

Authors: Soraya H. Foutouhi[1,2#], Nuradilla Mohamad-Fauzi[3#*], Dylan Bobby Storey[1†], Azarene A. Foutouhi[1], Nguyet Kong[1,2], Amir Kol[4], Dori Borjesson[4], Prerak Desai[1¶], Jigna Shah[1¶], James D. Murray[1,3*], and Bart C. Weimer[1,2*]

[1]*Department of Population Health and Reproduction,*

[2]*100K Pathogen Genome Project*

[3]*Department of Animal Science,*

[4]*Department of Pathology, Microbiology and Immunology,*

University of California, Davis, CA, USA. 95616

[#]co-first authors. Both contributed equally to this work.

Current Addresses: *University of Malaya, Institute of Ocean and Earth Sciences, Kuala Lumpur, Malaysia; [†]West Sacramento, CA; [¶]Janssen, Inc., Spring House, PN

[*]**Corresponding Authors**: Correspondence and requests for materials should be addressed to JDM (jdmurray@ucdavis.edu) and BCW (bcweimer@ucdavis.edu).

Author contributions:

SHF: Conception and design, Collection and/or assembly of data, Data analysis and interpretation, Manuscript writing; NMF: Conception and design, Collection and/or assembly of data, Data analysis and interpretation, Manuscript writing; DS: Informatics, Data analysis and interpretation; PD: Collection and/or assembly of data; JD: Collection and/or assembly of data; AAF: Administrative support, Collection and/or assembly of data; NK: Administrative support, Collection and/or assembly of data; AK: Collection and/or assembly of data, Data analysis and interpretation; DB: Study design, Provision of study material; JDM: Experiment conception and design, Financial support, Administrative support, Provision of study material, Data analysis and interpretation, Manuscript writing, Final approval of manuscript.; BCW: Experiment conception and design, Financial support, Administrative support, Provision of study material, Data analysis and interpretation, Manuscript writing, Final approval of manuscript.

bioRxiv preprint doi: https://doi.org/10.1101/795617; this version posted October 9, 2019. The copyright holder for this preprint (which was not certified by peer review) is the author/funder. All rights reserved. No reuse allowed without permission.

Abstract

The potential of mesenchymal stem cells (MSCs) for tissue repair and regeneration has garnered great attention. While MSC interaction with microbes at sites of tissue damage and inflammation is likely, especially in the gut, the consequences of bacterial association have yet to be elucidated. This study investigated the effect of *Salmonella enterica* ssp *enterica* serotype Typhimurium on MSC trilineage differentiation path and mechanism. Through examination of key markers of differentiation, immunomodulatory regulators, and inflammatory cytokines, we demonstrated that *Salmonella* altered osteogenic and chondrogenic differentiation pathways in human and goat adipose-derived MSCs. Gene expression profiles defined signaling pathway alterations in response to *Salmonella* association not observed in epithelial cells. We uncovered significant differential expression ($P < 0.05$) of genes associated with anti-apoptotic and pro-proliferative responses in MSCs during *Salmonella* challenge. These observations led us to conclude that bacteria, specifically *Salmonella,* induce pathways that influence functional differentiation trajectories in MSCs, thus implicating substantial microbial influence on MSC physiology and immune activity.

Introduction

Application of mesenchymal stem cells (MSCs) to regenerative medicine is an area of intensive research [1, 2]. In addition to a capacity for self-renewal and differentiation into cartilage, bone, and adipose tissue [3], MSCs home to sites of inflammation where they exhibit immunomodulatory functions via secretion of paracrine factors [4, 5]. In cooperation with recruited immune cells, MSCs moderate inflammation via expression of anti-inflammatory cytokines [6-8], inhibit T-lymphocyte activation, and alter macrophages to express a regulatory anti-inflammatory phenotype to increase phagocytic activity [5, 9]. Bacterial infections promote

bioRxiv preprint doi: https://doi.org/10.1101/795617; this version posted October 9, 2019. The copyright holder for this preprint (which was not certified by peer review) is the author/funder. All rights reserved. No reuse allowed without permission.

inflammation and prompts MSCs to secrete anti-microbial peptides [10].

Microbial access to MSCs is likely at mucus membranes where tissue turnover is high and immune-responsive cells infiltrate to control pathogens [11]. Inflammation, and subsequent destruction of intestinal epithelial cells induces MSC recruitment to facilitate tissue recovery [12]. While an apoptotic epithelial cell response to infection is well characterized [13], little is known about the consequences of bacterial association on the behavior of stem cells. Treatment of MSC with lipopolysaccharide (LPS) and *Escherichia coli* increases osteogenesis and decreases adipogenesis; conversely, stimulation with *Staphylococcus aureus* decreases osteogenesis and adipogenesis [14]. Recent discovery of invasion in MSCs by numerous bacteria common in the oral cavity and gut resulted in augmentation of MSC inhibition of T-cell proliferation and provides evidence of direct alteration of MSC immune function [15]. Maintenance of viability [15] and change in differentiation path [14] confirms that bacterial association with MSCs not only varies in comparison to epithelial cells, but also altered function beyond acute infection.

Host detection of microbial presence is accomplished in part by Toll-like receptors (TLRs), which recognize bacterial components on their cell surface in epithelial cells are also expressed in MSCs [16, 17]. It is not clear how pathogens regulate these molecules in MSCs. Tomchuck et al. [18] reported the promotion of MSC migratory abilities, whereas a study by Pevsner-Fischer [19] found TLR activation shifts lineage commitment to proliferation.

Salmonella pathogenesis in epithelial cells is primarily mediated via the type three-secretion system [20, 21], which injects effector proteins that lead to apoptosis. These proteins target a variety of host cell regulators, including the NFκB pathway, leading to an inflammatory environment that increases microbial internalization [21, 22]. Early transcription factors

bioRxiv preprint doi: https://doi.org/10.1101/795617; this version posted October 9, 2019. The copyright holder for this preprint (which was not certified by peer review) is the author/funder. All rights reserved. No reuse allowed without permission.

implicated in MSC differentiation such as, peroxisome proliferator-activated receptor gamma (PPARG) [23] and secreted phosphoprotein 1 (SPP1) [24], are involved in inflammation, and may bridge cellular response to microbe-induced inflammation in MSCs. Previously unexplored differences between the infectious route in epithelial cells and the immunomodulatory changes in MSCs during host-pathogen interaction suggest substantial stem cell conditioning by *Salmonella*. These novel observations led our group to hypothesize that microbial modulation of the immune system in MSCs provides pathogens with an uncharted method of tissue infiltration, resulting in undescribed biological impact.

In this study, it was hypothesized that human and goat MSCs internalize *Salmonella* that resulted MSC altered trajectories towards a pro-osteogenic commitment, in parallel with the induction of an anti-inflammatory, immunosuppressive cellular phenotype. Examination of differentiation markers, immunomodulatory regulators and inflammatory cytokines demonstrated that *Salmonella* was internalized without inducing MSC apoptosis that altered osteogenic and chondrogenic differentiation. This phenomenon extended to alter molecular mechanisms of cell survival, proliferation and immune regulation. These observations found microbial-specific alterations in MSC differentiation and inflammatory status to influence stem cell fate and functionality.

Materials and Methods

Cell culture

Human adipose-derived mesenchymal stem cells (hASCs) were isolated by the laboratory of Dr. Dori Borjesson (University of California, Davis) and cultured in Minimum Essential Medium Alpha Modification (MEM-α, HyClone) with 20% fetal bovine serum (FBS, HyClone) and 1% penicillin-streptomycin (P/S, Gibco Life Technologies). Goat adipose-derived mesenchymal

bioRxiv preprint doi: https://doi.org/10.1101/795617; this version posted October 9, 2019. The copyright holder for this preprint (which was not certified by peer review) is the author/funder. All rights reserved. No reuse allowed without permission.

stem cells (gASCs) were isolated by the laboratory of Dr. Matthew Wheeler (University of Illinois, Urbana-Champaign), as described by Monaco et al. [25], and expanded as described by Mohamad-Fauzi et al. [26]. ASCs were cultured in 5% CO_2/37°C, used at passage six. Colonic epithelial cells (Caco-2; ATCC HTB-37) were obtained from American Type Culture Collection (Manassas, VA) and grown as described by Shah et al. [27].

Bacteria culture

Salmonella enterica ssp *enterica* serotype Typhimurium LT2 (ST), 14028S, serotype Enteritidis (BCW_4673), serotype Saint Paul (BCW_88) and serotype Newport (BCW_1378) were grown in Luria-Bertani (LB) broth (Teknova, Holister, CA) and incubated with shaking (200 rpm) at 37°C. Cultures were grown as described by Kol et al. [15].

Quantification of microbe association

Association was determined using the gentamicin protection assay [28] and modified by Kol et al. [15], with the following modifications: ASCs were plated (4×10^4) in a 96-well plate and incubated overnight; bacteria were suspended in serum-free medium (10^8 CFU/ml) and added to the ASCs (MOI 100:1).

Transmission Electron Microscopy

hASCs were plated on glass slides (Nalge Nuc International, Naperville, IL) and incubated for 2 h with ST [15]. Preparation and completion of transmission electron microscopy (TEM) was conducted as outlined by Kol et al. [15].

Differentiation

Adipogenic and osteogenic differentiation was done using ASCs in 6-well plates at 2.5×10^5 ASCs/well and incubated with ST for 1 h as described above. Chondrogenic differentiation was done in T-25 flasks at 3×10^5 ASCs/flask. Following treatment with gentamicin, ASCs were

bioRxiv preprint doi: https://doi.org/10.1101/795617; this version posted October 9, 2019. The copyright holder for this preprint (which was not certified by peer review) is the author/funder. All rights reserved. No reuse allowed without permission.

121 washed with PBS and cultured for 48 hours in expansion medium to 70-80% confluence after
122 which differentiation medium was added.

123 **Osteogenic differentiation assay**

124 ASCs were cultured in osteogenic medium, fixed, rinsed and visualized under light and phase
125 microscopy as described in Mohamad-Fauzi et al. [26]. hASCs were cultured for 14 days,
126 whereas gASCs were cultured for 21 days. Control, non-induced cells were cultured in
127 expansion medium.

128 **Chondrogenic differentiation assay**

129 Chondrogenic differentiation was carried out as described by Zuk et al. [29]. Following ST
130 incubation, 70-80% confluent cells were trypsinized and suspended in expansion medium for 14
131 days and then processed and visualized as described by Mohamad-Fauzi et al. [26].

132 **Adipogenic differentiation assay**

133 Cells were cultured for 21 days in adipogenic induction medium, fixed, stained, and visualized as
134 described by Mohamad-Fauzi et al. [26].

135 **RNA extraction and cDNA synthesis**

136 ASCs were flash frozen prior to RNA extraction. For analysis of immunomodulatory factors,
137 ASCs were plated in 6-well plates (3×10^5 cells/well) and incubated with ST as described above.
138 Treatment with LPS (Sigma) was added at 10 ng/ml. MSCs were washed with PBS, and
139 immediately lysed with TRIzol Reagent (Life Technologies). Total RNA was extracted as
140 described by Mohamad-Fauzi et al. [26]. Total RNA (1 µg) was used for first-strand cDNA
141 synthesis using SuperScript II Reverse Transcriptase (Life Technologies) and oligo-dT primers
142 according to the manufacturer.

bioRxiv preprint doi: https://doi.org/10.1101/795617; this version posted October 9, 2019. The copyright holder for this preprint (which was not certified by peer review) is the author/funder. All rights reserved. No reuse allowed without permission.

Quantitative RT-PCR

Primers (Supplementary Tables 1-2) were designed using Primer3 if not obtained from references. All primers spanned exon junctions or included introns. mRNA expression was quantified using Fast SYBR Green reagent (Life Technologies) on the Bio-Rad CFX96 platform (95°C for 20 seconds, 40 cycles of 95°C for 3 s and 60°C for 30 s), followed by melt curve analysis. Gene expression was normalized to GAPDH using $2^{-\Delta\Delta CT}$ [30, 31]. Differences in differentiation gene expression were calculated as fold-changes relative to cells cultured in expansion medium (non-induced) and not treated with bacteria (non-treated). Inflammatory gene expression was calculated as fold-changes relative to non-treated control cells. Treatments were analyzed in pairwise comparisons using the Student's t-test on the software JMP (SAS Institute) ($p \leq 0.05$). Data are presented as mean ± SEM with three biological and technical replicates.

GeneChip expression analyses

Caco-2 infection samples with *Salmonella* LT2 were conducted using Affymetrix HGU133Plus2 GeneChip. Custom arrays containing all annotated coding and intergenic sequences of *Salmonella enterica* spp. *enterica* sv Typhimurium LT2 [32-34]. Data were normalized using MS-RMA [35] and analyzed using Significance Analysis of Microarrays (SAM) [33, 36].

hASC RNA sequencing

Total RNA (1 µg) from hASCs was used to construct sequencing libraries with the Truseq Stranded Total RNA LT Kit (Illumina). Quality of RNA and constructed libraries was determined via 2100 Bioanalyzer. Libraries sequenced using an Illumina HiSeq2000 (BGI@UC Davis, Sacramento, CA) with single-end 50 bp. Reads were aligned using the UCSC hg19 human reference genome (ftp://igenome:G3nom3s4u@ussd-ftp.illumina.com/Homo_sapiens/UCSC/hg19/Homo_sapiens_UCSC_hg19.tar.gz) and annotated

bioRxiv preprint doi: https://doi.org/10.1101/795617; this version posted October 9, 2019. The copyright holder for this preprint (which was not certified by peer review) is the author/funder. All rights reserved. No reuse allowed without permission.

using "-a 10 --b2-very-sensitive -G". Read counts and normalization was done using Cufflinks package (version 2.2.0) with flags "-u -G". Tables from cuffnorm and cuffdiff imported into Ingenuity Pathway Analysis (IPA; Ingenuity Systems, version spring 2014). Sequence quality was examined using Phred [Supplementary Figure S1A-B].

Ingenuity Pathway Analysis

IPA was used to determine biological pathways associated with gene expression profiles. Networks represent molecular interaction based on the IPA knowledge database. Estimation of probable pathway association was determined Fisher's exact test, and predicted direction change was decided by the IPA regulation z-score algorithm (z-score ≥ 2 and ≤ 2 means a function is significantly increased or decreased, respectively) [37].

Results

Microbial association with adipose-derived mesenchymal stem cells

Human and goat ASCs were susceptible to *Salmonella* infection *in vitro* [Figure 1], which recapitulated previous observations in canine ASCs [15]. Total associated bacteria in both organisms were invasive; gASCs showed significantly higher invasion compared to human cells ($P = 0.006$) [Figure 1A]. Microbial association was not exclusive to ST; other *Salmonella* serotypes also invaded ASCs, as did other organisms as our group demonstrated previously [15], signifying a consistent trend in ASC vulnerability to common pathogens [Figure 1B]. Utilizing TEM, intracellular ST were observed 2 h post hASC-microbe co-incubation [Figure 1C-F]. Cells were not morphologically distressed nor apoptotic. In addition to invasion, ST adherence to hASC cell surface was observed; this intimate association is consistent with other non-pathogenic bacteria that Kol et al. [15] also observed.

As ST is the most common cause of enteric diarrhea, we limited additional studies to this

bioRxiv preprint doi: https://doi.org/10.1101/795617; this version posted October 9, 2019. The copyright holder for this preprint (which was not certified by peer review) is the author/funder. All rights reserved. No reuse allowed without permission.

serotype. Following ST co-incubation, the expression of several immunomodulatory genes was investigated [Figure 1G-H]. Interleukin 8 and 6 (*IL8*, *IL6*), prostaglandin-endoperoxide synthase 2 (*PTGS2*), nuclear factor of kappa light polypeptide gene enhancer in B-cells 1 (*NFKB1*), transforming growth factor beta 1 (*TGFB1*), *PPARG* and *SPP1* were selected. gASCs and hASCs treated with ST significantly increased *IL8* expression ($P \leq 0.033$, $P \leq 0.005$, respectively). An increase in *IL8* was also observed in LPS-treated gASCs ($P \leq 0.0001$). LPS-stimulated gASCs induced a significant increase in *IL6* ($P = 0.0001$), *PTGS2* ($P = 0.0009$), *NFKB1* ($P = 0.0002$), *PPARG* ($P = 0.0204$), *SPP1* ($P = 0.037$) and *IL8* ($P \leq 0.0001$) gene expression.

A broader analysis of gene expression using RNAseq found 118 significantly differentially expressed genes in ST/hASCs interactions ($P \leq 0.05$, FDR = 0.1). Canonical pathway analysis found hASCs treated with ST repressed cell death and survival genes associated with apoptosis [Figure 2]. TNF/FasL pathway analysis [Figure S2] established the muted apoptotic response in hASCs compared to Caco-2 cells following ST infection. Consistent with viability post ST association, induced genes in hASCs included repression of apoptosis, promotion of proliferation and multipotency [Figure 3.1]. Expression of heat shock protein B6 (*HSPB6*) and MAP-predicted activation of *v-akt* murine thymoma viral oncogene homolog 1 (*AKT1*) indicate promotion of hASC survival. *HSPB6* inhibits apoptosis of murine tumor cells, and plays a role in cellular protection against oxidative damage [38, 39]. Activated in response to a variety of cues, *AKT1* helps mediate cell survival and clonogenic potential [40-43].

Upregulated in ST-treated hASCs [Figure 3.1], parathymosin (*PTMS*) is involved in molecular organization, differentiation and proliferation; nuclear translocation of *PTMS* is indicative of a pro-proliferative state [44, 45]. MAP predicted the repression of hedgehog

bioRxiv preprint doi: https://doi.org/10.1101/795617; this version posted October 9, 2019. The copyright holder for this preprint (which was not certified by peer review) is the author/funder. All rights reserved. No reuse allowed without permission.

signaling (Hh), whose inhibition is reported to decrease MSC proliferation with no effect on differentiation capacity [46]. We observed an increase in expression of patched 2 (*PTCH2*), which influences epidermal differentiation and Hh activity, suggesting promotion of ASC proliferation [47].

Superoxide dismutase 3 (*SOD3*) is pivotal for management of cellular redox [48-50] and was induced in this study [Figure 3.2], which aligns with previous observations in INFγ/LPS-activated microglial cells [48]. By promoting phagocytosis, EC-SOD facilitates bacteria clearance and elicits an anti-inflammatory response to LPS induced inflammation and pulmonary infection [51-53]. Interestingly, while Caco-2 cells strongly induced expression of TLR signaling which facilitates the LPS response following pathogen challenge, this observation was not seen in hASCs [Figure S3]. Using MAP, we focused on upstream regulators of *SOD3*, which may have been responsible for its activation [Figure 3.2]. Both *SOX10* and heparin sulfate (HS), play a role in the maintenance of multipotency and self-renewal [54, 55]. Interferon gamma (*INFG*) influences the immunomodulatory effects of MSC, as *INFG*-activated MSCs suppress T-cells and provide the necessary signal for MSC immunosuppression [56].

Analysis of trilineage differentiation post-microbial association Chondrogenic Differentiation

ST treatment did not abate ASCs ability to undergo chondrogenesis. In hASCs, differentiated cells migrated to form ridges that stained with Alcian Blue [Figure 4.2]. The morphological changes in gASCs were more advanced compared to human cells after ridge formation, cells aggregated, forming clumps that stained positive with Alcian Blue. Control, non-induced cells remained in monolayer and exhibited minimal background staining.

Expression of SRY (sex determining region Y)-box 9 (*SOX9*), which is essential for

bioRxiv preprint doi: https://doi.org/10.1101/795617; this version posted October 9, 2019. The copyright holder for this preprint (which was not certified by peer review) is the author/funder. All rights reserved. No reuse allowed without permission.

cartilage formation [57] and encodes for a transcription factor that promotes cartilage-specific extracellular matrix components [58, 59], was measured 14-days post chondrogenic induction. In hASCs, *SOX9* expression decreased ($P = 0.04$) in cells treated with ST [Figure 5.2]. Non-induced hASCs treated with ST showed no significant change in *SOX9* expression. Chondrogenic induction increased *SOX9* expression in hASCs compared to cells treated with control medium ($P = 0.034$). gASCs showed a significant decrease in *SOX9* expression in induced and non-induced ST-treated cells ($P = 0.027$, $P = 0.039$). There was a significant decrease in *SOX9* expression between gASCs treated with induction ($P = 0.012$).

Adipogenic Differentiation

ASCs cultured in adipogenic medium accumulated lipid-filled vacuoles that stained with Oil Red O [Figure 4.3]. Visually, no differences were observed between non-induced ST-treated cells and the controls, which did not yield lipid-filled adipocytes nor stain with Oil Red O.

The lack of visual differentiation was further explored by examining expression of *PPARG* and fatty acid binding protein 4 (*FABP4*) 21 days post-induction, which should detect early events in adipogenesis [60, 61]. ST treatment of induced and non-induced hASCs did not change *PPARG* expression [Figure 5.3], a trend consistent with gASCs; however, a significant increase in *PPARG* expression in human and goat ASCs treated with differentiation vs. control medium ($P \leq 0.0001$, $P \leq 0.0001$) was observed, as expected.

FABP4 is a fatty acid binding protein specific to mammalian adipose tissue [62, 63]. No significant difference was observed between induced ASCs treated with ST and non-treated control cells. Non-induced hASCs, but not gASCs, treated with ST displayed a significant increase in *FABP4* expression ($P = 0.019$). Both species induced *FABP4* in cells cultured in adipogenic induction medium [Figure 5.3] ($P = 0.029$, $P \leq 0.0001$).

bioRxiv preprint doi: https://doi.org/10.1101/795617; this version posted October 9, 2019. The copyright holder for this preprint (which was not certified by peer review) is the author/funder. All rights reserved. No reuse allowed without permission.

Osteogenic Differentiation

ASCs induced with osteogenic medium post ST treatment underwent osteogenesis. Mineralized calcium deposits accumulated within the monolayer and stained with Alizarin Red S [Figure 4.1]. By visual comparison, no difference was apparent between ST-treated and non-treated cells. ASCs cultured in control, expansion medium did not undergo calcium mineralization nor stain with Alizarin Red S, independent of ST treatment [Figure 4.1].

Collagen type I alpha 1 (*COL1A1*), alkaline phosphatase (*ALPL*) and *SPP1* expression were determined at the termination of differentiation. *COL1A1* encodes for the major component of the most abundant collagen found in bone matrix [64]. In hASCs induced for osteogenesis, *COL1A1* expression was significantly higher in ST-treated cells compared to controls ($P = 0.025$) [Figure 5.1A]. No difference in expression was detected between non-induced ST-treated and control hASCs. There was a significant decrease in *COL1A1* expression in hASCs treated with osteogenic induction vs. control medium ($P \leq 0.0001$). gASCs displayed no significant change of *COL1A1* expression in induced ST treated cells [Figure 5.1B]. There was a significant decrease in *COL1A1* expression between gASCs treated with osteogenic induction vs. control medium ($P = 0.018$).

ALPL, which provides phosphate ions for the production of bone mineral during matrix maturation [65-67], increased in induced hASCs ($P = 0.02$) as well as ST treated-induced hASCs. *ALPL* expression was 3.3-fold higher than in non-treated cells ($P = 0.03$) [Figure 5.1A]. In non-induced hASCs, no significant change in *ALPL* expression was detected following ST-treatment. *ALPL* expression in gASCs was not detected.

SPP1 is a non-collagenous bone protein expressed during the mineralization phase late in osteogenesis [68]. In hASCs, *SPP1* was repressed in induced cells ($P \leq 0.0001$). *SPP1*

bioRxiv preprint doi: https://doi.org/10.1101/795617; this version posted October 9, 2019. The copyright holder for this preprint (which was not certified by peer review) is the author/funder. All rights reserved. No reuse allowed without permission.

281 expression was 4.3-fold higher in induced hASCs treated with ST compared to non-treated cells
282 ($P = 0.002$). In non-induced hASCs, no difference in expression was observed between ST-
283 treated and control cells [Figure 5.1A]. In induced gASCs, no significant change in SPP1
284 expression was observed in ST-treated cells. However, a 7.2-fold increase in SPP1 was observed
285 in non-induced gASCs treated with ST compared to non-treated, non-induced controls ($P \leq 0.05$)
286 [Figure 5.1B].

287 Pretreatment of hASCs with ST followed by 14 days of osteogenic induction resulted in
288 the differential expression of 1060 genes (data not shown). RNAseq-IPA regulation z-score
289 algorithm identified associated downstream biological functions. Expression data projected the
290 repression of genes associated with cell-to-cell signaling, inflammation and response to
291 infectious disease [Figure 6.1], highlighting the potential anti-inflammatory phenotype of hASCs
292 subjected to microbial association (P-value ≤ 0.05, z-score ≥ 2).

293 ST treatment followed by osteogenic differentiation also influenced genes involved in
294 cellular communication, migration and lineage commitment. Differentially expressed genes
295 included stanniocalcin 1 (*STC1*) and mesenchyme homeobox 2 (*MEOX2*) [Figure 6.2]. MSCs
296 secrete *STC1* in response to apoptotic signals [69]. *STC1* is reported to play a role in the
297 suppression of inflammation and may act in the regulation of calcium and phosphate homeostasis
298 [69, 70]. *STC1* expression was downregulated in differentiated hASCs pre-treated with ST.

299 Upregulated in ST treated osteogenic differentiated hASCs [Figure 6.2], chloride
300 intracellular channel 4 (*CLIC4*) is induced during cellular stress and influences cell cycle arrest
301 and apoptosis [71]. Intracellular chloride regulates cation transport and may be involved in
302 cellular signaling; *CLIC4* expression has been reportedly associated with Ca^{2+} induced
303 differentiation of keratinocytes [71, 72]. Macrophage migration inhibitory factor (MIF) is

bioRxiv preprint doi: https://doi.org/10.1101/795617; this version posted October 9, 2019. The copyright holder for this preprint (which was not certified by peer review) is the author/funder. All rights reserved. No reuse allowed without permission.

304 elevated during tissue injury and inhibits MSC migration [73, 74]. Our data showed
305 downregulation of MIF expression [Figure 6.2]. Furthermore, adhesion to fibronectin through
306 α5β1-integrin plays a part in the induction of MSC migration [75]. MSC expression of A1-3, B1,
307 and B3/4 integrins has been reported; blocking of B1 decreased migration in bone marrow-
308 derived MSCs [76, 77]. We detected an increase in A3, A4 and B1 integrins [Figure S5].
309 Induction of periostin (*POSTN*) following ST challenge [Figure 6.2] was observed. A
310 regulator of Wnt/β-catenin signaling cascade and mediator of bone anabolism, *POSTN* increases
311 in response to stress and tissue damage [78, 79]. Wnt pathway activity is regulated by
312 extracellular factors, including heparin sulfate proteoglycans, and acts to control MSC
313 proliferation and differentiation [80]. hASCs treated with ST prior to induction displayed
314 downregulation of Wnt activator Secreted frizzled-related protein 1 (*SFRP1*) and induction of
315 transcription factors *JUN* and *AXIN2* [Figure S4A]. In addition, we observed a marked increase
316 in the expression of *TNFRSF11B* [Figure S4B]. Also known as osteoprotegerin, *TNFRSF11B* is
317 an anti-osteoclastogenic regulator, which is reported to augment osteogenesis [81].
318 Ephrin-B2 (*EFNB2*) is involved in osteogenic commitment and is required for
319 differentiation of osteoclasts and osteoblasts *in vivo* [82]. Upregulated in our data set [Figure
320 6.2], the *EFNB2* ligand and *EPHB4* receptor are reportedly expressed on the surface of MSCs
321 [82]. Increased expression of *COL1A2* was also detected [Figure 6.2]. *COL1A2* promotes cellular
322 proliferation and osteogenesis, a response in part regulated by ERK/AKT1 pathway activation
323 [83]. Activation of ERK mitogen activated protein kinase family (*MAPK*) drives the progression
324 of osteoblasts via phosphorylation of transcription factors [77]. Overlay of hASC gene
325 expression data illustrated upregulation of integrins involved in *MAPK1* activation as well as
326 intracellular signal transducer phosphatidylinositol-4,5-bisphosphate 3-kinase (*PI3K*) [Figure

bioRxiv preprint doi: https://doi.org/10.1101/795617; this version posted October 9, 2019. The copyright holder for this preprint (which was not certified by peer review) is the author/funder. All rights reserved. No reuse allowed without permission.

S5].

Consistent with MSC ability to influence the immune response, we detected expression of genes involved in MSC signaling and immunomodulation [Figure 6.2]. Cadherin 11 (*CDH11*) expression was upregulated in our dataset. TGFB treatment increases expression of *CDH11* and subsequent calcium-dependent cell-to-cell interactions in MSCs [84]. Engagement of *CDH11* on fibroblast-like synoviocytes (FLS) has been reported to produce inflammatory mediators IL6 and IL8 [84], though our transcriptome analysis did not indicate significant upregulation of either of these cytokines. Kol et al. demonstrated that ST augments cMSCs ability to inhibit T-cell proliferation [15]. In hASCs, we observed the differential expression of genes involved in the suppression of immune cells; IPA regulator analysis highlighted the potential inhibitory effect of ST-treated hASCs on phagocyte and granulocyte proliferation [Figure S6].

Discussion

Microbial presence on host tissue presents a wide range of beneficial to pathogenic effects on cellular function. Intestinal bacteria have been shown to contribute to cellular proliferation and development; observation of host and microbe interactions during inflammatory and disease states have been imperative in refining our understating of healing and self-renewal signaling mechanisms [85]. Studies on pathogen interference on MSC functionality demonstrate the promising potential of stem cells as a mode of intercession for infection and inflammation. Yuan et al [86] illustrated the ability of bone marrow-derived MSCs to increase clearance of methicillin-resistant *Staphylococcus aureus* (MRSA) in a rat model; work by Maiti and colleagues show that MSC stimulation with MRSA resulted not only in changes to cell proliferation but also the induction of inflammatory markers [87]. Here, ASCs were susceptible to microbial infection *in vitro* with many types of *Salmonella*, suggesting this is a common

bioRxiv preprint doi: https://doi.org/10.1101/795617; this version posted October 9, 2019. The copyright holder for this preprint (which was not certified by peer review) is the author/funder. All rights reserved. No reuse allowed without permission.

characteristic, especially when taken with the observations of Kol et al. [15]. Our specific investigation of ST resulted in changes in the expression of prototypical gene markers of differentiation and inflammation, but not apoptosis.

Fiedler et al. [14] found continuous treatment with heat-inactivated *E. coli* slightly increased ALPL activity in hASCs; heat-inactivation may have diminished the effect of bacterial exposure. The migration of MSCs to sites of inflammation, where bacterial interaction may be transient, could potentiate a narrow window of opportunity for microbial association. The use of viable bacteria and shorter exposure time in this study may better mimic the physiological conditions in which MSCs interact with microbes. We observed internalization of ST within 60 minutes of co-incubation; additional investigation is required to evaluate ST presence throughout extended culture periods. ST pre-treatment did not abate the ability of ASCs to differentiate, but did affect the expression of genes involved in osteogenesis and chondrogenesis.

ST treatment had a significant effect on osteogenic differentiation. In congruence with Fiedler et al. [14], we observed an increase in *ALPL* expression in ST-treated hASCs induced for osteogenesis. Increase in *ALPL* expression is consistent with the finding at 10 days post-osteogenic induction in LPS-treated hASCs [16]. *ALPL* was not detected in gASCs, as cells were harvested 21 days post-induction when the mineralization phase was likely occurring [88] and *ALPL* expression may have decreased [67, 88].

Consistent with the lack of *ALPL*, upregulation of *SPP1* (a late marker of osteogenesis) [88, 89], was observed in ST-treated gASCs. In addition to osteogenic commitment, the 6-glycosylated phosphoprotein SPP1 has a significant role in cellular stress and immunity. As an inflammatory mediator, SPP1 is reported as anti-inflammatory in acute colitis, while having an opposite effect in chronic disease status [90, 91]. Plasma levels of SPP1 are elevated in Crohn's

bioRxiv preprint doi: https://doi.org/10.1101/795617; this version posted October 9, 2019. The copyright holder for this preprint (which was not certified by peer review) is the author/funder. All rights reserved. No reuse allowed without permission.

disease and SPP1-deficient mice have an impaired ability to clear *Listeria monocytogenes* [90, 92]. The upregulation of *SPP1* observed implies a diverse series of biological effect on MSC physiology. It is probable that the involvement of SPP1 in response to microbe-induced inflammation results in the influence of ASCs towards osteogenesis.

Differential marker expression following ST treatment was heavily observed in non-induced ASCs. Upregulation of *SPP1* was observed in ST-treated, non-induced gASCs, but not in induced cells. It is possible that the osteoinductive effect of ST treatment in induced ASCs was masked, as the medium contained additives that strongly induce osteogenesis. Pevsner-Fischer et al. [19] observed a differential effect of LPS treatment on non-induced MSCs compared to induced. Thus, the upregulation of osteogenic markers in non-induced cells highlight the direct influence of microbial treatment on ASC lineage commitment.

We observed a concomitant decrease in chondrogenic differentiation in response to ST treatment, as shown by a decrease in *SOX9* expression in ASCs. To our knowledge, this is the first report on the direct effect of bacterial association on MSC chondrogenesis. SOX9 is required for commitment to chondrogenic lineage, thus murine *SOX9*-null cells do not express markers of chondrogenesis [93]. Osteogenesis and chondrogenesis are tightly coupled processes [94], both regulated by proteins in the TGFβ superfamily [95]. An inverse relationship between osteogenic and chondrogenic differentiation has been demonstrated; microRNAs targeting genes important for osteogenesis were upregulated during chondrogenesis, and vice versa [96]. This further supports the premise that ASCs pre-exposed to ST prior to induction favor characteristics of osteogenic lineage commitment.

Exposure to whole bacteria and microbial components are sufficient to influence ASC signaling. MSC response to microbial components is mediated by Toll-like receptors (TLRs);

bioRxiv preprint doi: https://doi.org/10.1101/795617; this version posted October 9, 2019. The copyright holder for this preprint (which was not certified by peer review) is the author/funder. All rights reserved. No reuse allowed without permission.

hASCs express *TLR1-6* and *TLR9* [16]. TLR4 agonist LPS is a key component of the *Salmonella* cell wall [97]. LPS influences osteogenesis in hASCs and bone marrow-derived MSCs (BM-MSCs) by increasing mineralization, ALP activity, and expression of osteogenic markers [14, 16, 98, 99]. It is possible that LPS-induced changes in differentiation are mediated by TLRs and thus, dependent on NFKB1 activation [99, 100]. In this study, we did not observe upregulation of *NFKB1* expression following ST challenge or significant induction of genes involved in TLR signaling pathway. As a rapid responder, NFKB1 proteins are available and inactive; activity depends on phosphorylation-dependent degradation of NFKB1 inhibitors, thus the lack of change in mRNA expression is not unexpected [101].

While the conditions of this study did not lead to an observed induction of TLR gene expression, previous reports highlight the role of TLR activation in MSC physiology. TLR2 activation inhibited spontaneous adipogenic differentiation and increased osteogenesis in non-induced mouse BM-MSCs, but inhibits trilineage differentiation in induced cultures [19]. The upregulation of osteogenic markers in non-induced ST treated ASCs in this study supports this observation. Furthermore, TLR-activated MSCs recruit immune cells; TLR-activated macrophages secreted oncostatin M, a cytokine that induces osteogenic and inhibits adipogenesis in BM-MSCs [102]. MSCs deficient in myeloid differentiation primary response 88 (*MYD88*), which is crucial for TLR signaling [103], lack both osteogenic and chondrogenic potential [19], providing further evidence for linking microbe-induced TLR signaling and osteochondrogenic pathway induction.

Initiation of epithelial inflammation and rapid induction of pro-inflammatory cytokines via calcium-mediated activation of NFKB1 in response to *Salmonella* is documented [104, 105]. A dose-dependent increase in IL8 secretion was reported in human BM-MSCs following LPS

bioRxiv preprint doi: https://doi.org/10.1101/795617; this version posted October 9, 2019. The copyright holder for this preprint (which was not certified by peer review) is the author/funder. All rights reserved. No reuse allowed without permission.

419 treatment [106]. A hallmark of IL8 is the capacity for a variety of cells, including MSCs, to
420 rapidly express and secrete IL8 [107]. IL8 can inhibit osteoclasts bone resorption activity, and
421 stimulates osteoclast motility [108, 109]. Upregulation of *IL8* was detected after 14 days of
422 osteogenic media treatment [108]. In additional support of the coordination between
423 inflammatory and differentiation pathways, co-incubation with ST significantly increased *IL8*
424 expression in hASCs and gASCs.

425 Coordination between inflammation and lineage commitment likely involves various
426 small molecules. A pleiotrophic cytokine, IL6 is involved in innate tissue response to injury and
427 maintenance of undifferentiated MSCs status, and *IL6* expression decreases during osteogenic
428 differentiation [110]. While mature osteoblasts displayed enhanced osteogenic differentiation,
429 primitive MSCs experienced a decrease in proliferation following IL6 treatment [111], implying
430 that IL6 influence on osteogenesis is complex and dependent on the status of targeted MSCs. In
431 this study, a significant increase in *IL6* expression was observed in LPS-treated gASCs. A
432 similar trend was noted in ST-treated gASCs and hASCs, although not statistically significant.
433 This suggests that ASC response to ST infection influences the secretion of small molecules
434 capable of cross-talk between inflammatory and differentiation pathways.

435 The transcriptome of hASCs post ST association alludes to a physiological shift in favor
436 of cell survival and proliferation. Under oxidative stress, MSCs display a reduced ability to
437 repair tissue and an increased propensity towards senescence [112, 113]. These conditions
438 decrease MSC capacity for osteogenesis in favor of adipogenic commitment [113]. Through
439 upregulation of redox mediators, hASCs appear to respond and mitigate oxidative stress, helping
440 to insure cell viability, multipotency, and promote immune suppression. As versatile immune
441 privileged cells, MSCs presented with microbial challenge may function as a safeguard,

bioRxiv preprint doi: https://doi.org/10.1101/795617; this version posted October 9, 2019. The copyright holder for this preprint (which was not certified by peer review) is the author/funder. All rights reserved. No reuse allowed without permission.

442 contributing to an anti-inflammatory environment, which allows time and an atmosphere
443 conducive for infection clearance by resident phagocytes. However, it is unlikely that hASC
444 response to ST is without physiological consequences, as influence of inflammatory mediators
445 on lineage commitment appears to prime hASCs towards a pro-osteogenic phenotype.

446 The direct association of ASCs with ST influences key modulators of trilineage
447 differentiation. We illustrate that, as the pathways dictating MSC response to injury, microbial
448 products and inflammation overlap with the regulation of cellular differentiation, exposure to
449 bacteria alters lineage commitment. However, the extent and mechanisms responsible for
450 eliciting changes in MSC differentiation due to microbial interaction have yet to be fully
451 described. As ASCs are currently in contention as a powerful model for understanding the
452 complex interaction of pathogenesis, inflammation and calcification, further investigation into
453 the complex relationship between bacterial association and ASC physiology is imperative, as we
454 have established that this association results in distinctive changes to MSC physiology.

455 **Acknowledgments**

456 We thank Majlis Amanah Rakyat (Malaysia) and the Jastro Shields Research Fellowship,
457 and the USDA-CREES W2171 Regional Research Project for funding a portion of the work
458 described in this paper (NMF).

459

bioRxiv preprint doi: https://doi.org/10.1101/795617; this version posted October 9, 2019. The copyright holder for this preprint (which was not certified by peer review) is the author/funder. All rights reserved. No reuse allowed without permission.

460 **References:**

461 1. Fossett, E. and W.S. Khan, *Optimising human mesenchymal stem cell numbers for*
462 *clinical application: a literature review.* Stem Cells Int, 2012. **2012**: p. 465259.
463 2. Marra, K.G. and J.P. Rubin, *The potential of adipose-derived stem cells in craniofacial*
464 *repair and regeneration.* Birth Defects Res C Embryo Today, 2012. **96**(1): p. 95-7.
465 3. Dominici, M., et al., *Minimal criteria for defining multipotent mesenchymal stromal*
466 *cells. The International Society for Cellular Therapy position statement.* Cytotherapy,
467 2006. **8**(4): p. 315-7.
468 4. Ortiz, L.A., et al., *Mesenchymal stem cell engraftment in lung is enhanced in response to*
469 *bleomycin exposure and ameliorates its fibrotic effects.* Proc Natl Acad Sci U S A, 2003.
470 **100**(14): p. 8407-11.
471 5. Balaji, S., S.G. Keswani, and T.M. Crombleholme, *The Role of Mesenchymal Stem Cells*
472 *in the Regenerative Wound Healing Phenotype.* Adv Wound Care (New Rochelle), 2012.
473 **1**(4): p. 159-165.
474 6. Roddy, G.W., et al., *Action at a distance: systemically administered adult*
475 *stem/progenitor cells (MSCs) reduce inflammatory damage to the cornea without*
476 *engraftment and primarily by secretion of TNF-alpha stimulated gene/protein 6.* Stem
477 Cells, 2011. **29**(10): p. 1572-9.
478 7. Galindo, L.T., et al., *Mesenchymal stem cell therapy modulates the inflammatory*
479 *response in experimental traumatic brain injury.* Neurol Res Int, 2011. **2011**: p. 564089.
480 8. Romieu-Mourez, R., et al., *Cytokine modulation of TLR expression and activation in*
481 *mesenchymal stromal cells leads to a proinflammatory phenotype.* J Immunol, 2009.
482 **182**(12): p. 7963-73.
483 9. Eggenhofer, E. and M.J. Hoogduijn, *Mesenchymal stem cell-educated macrophages.*
484 Transplant Res, 2012. **1**(1): p. 12.
485 10. Krasnodembskaya, A., et al., *Antibacterial effect of human mesenchymal stem cells is*
486 *mediated in part from secretion of the antimicrobial peptide LL-37.* Stem Cells, 2010.
487 **28**(12): p. 2229-38.
488 11. Xu, X.R., et al., *Dysregulation of mucosal immune response in pathogenesis of*
489 *inflammatory bowel disease.* World J Gastroenterol, 2014. **20**(12): p. 3255-64.
490 12. Semont, A., et al., *Mesenchymal stem cells increase self-renewal of small intestinal*
491 *epithelium and accelerate structural recovery after radiation injury.* Adv Exp Med Biol,
492 2006. **585**: p. 19-30.
493 13. Kim, J.M., et al., *Apoptosis of human intestinal epithelial cells after bacterial invasion.* J
494 Clin Invest, 1998. **102**(10): p. 1815-23.
495 14. Fiedler, T., et al., *Impact of bacteria and bacterial components on osteogenic and*
496 *adipogenic differentiation of adipose-derived mesenchymal stem cells.* Exp Cell Res,
497 2013. **319**(18): p. 2883-92.
498 15. Kol, A., et al., *Gastrointestinal microbes interact with canine adipose-derived*
499 *mesenchymal stem cells in vitro and enhance immunomodulatory functions.* Stem Cells
500 Dev, 2014. **23**(16): p. 1831-43.
501 16. Hwa Cho, H., Y.C. Bae, and J.S. Jung, *Role of toll-like receptors on human adipose-*
502 *derived stromal cells.* Stem Cells, 2006. **24**(12): p. 2744-52.
503 17. Raicevic, G., et al., *Inflammation modifies the pattern and the function of Toll-like*
504 *receptors expressed by human mesenchymal stromal cells.* Hum Immunol, 2010. **71**(3):

bioRxiv preprint doi: https://doi.org/10.1101/795617; this version posted October 9, 2019. The copyright holder for this preprint (which was not certified by peer review) is the author/funder. All rights reserved. No reuse allowed without permission.

p. 235-44.
18. Tomchuck, S.L., et al., *Toll-like receptors on human mesenchymal stem cells drive their migration and immunomodulating responses.* Stem Cells, 2008. **26**(1): p. 99-107.
19. Pevsner-Fischer, M., et al., *Toll-like receptors and their ligands control mesenchymal stem cell functions.* Blood, 2007. **109**(4): p. 1422-32.
20. Rivera-Chavez, F., et al., *Salmonella uses energy taxis to benefit from intestinal inflammation.* PLoS Pathog, 2013. **9**(4): p. e1003267.
21. Pilar, A.V., et al., *Active modification of host inflammation by Salmonella.* Gut Microbes, 2013. **4**(2): p. 140-5.
22. Thiennimitr, P., S.E. Winter, and A.J. Baumler, *Salmonella, the host and its microbiota.* Curr Opin Microbiol, 2012. **15**(1): p. 108-14.
23. Pascual, G., et al., *A SUMOylation-dependent pathway mediates transrepression of inflammatory response genes by PPAR-gamma.* Nature, 2005. **437**(7059): p. 759-63.
24. Sabo-Attwood, T., et al., *Osteopontin modulates inflammation, mucin production, and gene expression signatures after inhalation of asbestos in a murine model of fibrosis.* Am J Pathol, 2011. **178**(5): p. 1975-85.
25. Monaco, E., et al., *Morphological and transcriptomic comparison of adipose and bone marrow derived porcine stem cells.* The Open Tissue Engineering & Regenerative Medicine Journal, 2009. **2**: p. 20-33.
26. Mohamad-Fauzi, N., et al., *Impact of source tissue and ex vivo expansion on the characterization of goat mesenchymal stem cells.* J Anim Sci Biotechnol, 2015. **6**(1): p. 1.
27. Shah, J., P.T. Desai, and B.C. Weimer, *Genetic mechanisms underlying the pathogenicity of cold-stressed Salmonella enterica serovar typhimurium in cultured intestinal epithelial cells.* Appl Environ Microbiol, 2014. **80**(22): p. 6943-53.
28. Elsinghorst, E.A., *Measurement of invasion by gentamicin resistance.* Methods Enzymol, 1994. **236**: p. 405-20.
29. Zuk, P.A., et al., *Multilineage cells from human adipose tissue: implications for cell-based therapies.* Tissue Eng, 2001. **7**(2): p. 211-28.
30. Livak, K.J. and T.D. Schmittgen, *Analysis of relative gene expression data using real-time quantitative PCR and the 2(-Delta Delta C(T)) Method.* Methods, 2001. **25**(4): p. 402-8.
31. Schmittgen, T.D. and K.J. Livak, *Analyzing real-time PCR data by the comparative C(T) method.* Nat Protoc, 2008. **3**(6): p. 1101-8.
32. Shah, J., et al., *Preadaptation to cold stress in Salmonella enterica serovar Typhimurium increases survival during subsequent acid stress exposure.* Appl Environ Microbiol, 2013. **79**(23): p. 7281-9.
33. Ng, K.M., et al., *Microbiota-liberated host sugars facilitate post-antibiotic expansion of enteric pathogens.* Nature, 2013. **502**(7469): p. 96-9.
34. Marcobal, A., et al., *Bacteroides in the infant gut consume milk oligosaccharides via mucus-utilization pathways.* Cell Host Microbe, 2011. **10**(5): p. 507-14.
35. Stevens, J.R., Balasubramanian Ganesan, Prerak Desai, Sweta Rao, and Bart C. Weimer. . *Statistical issues for normalization of multi-species microarray data.* . in *Nineteenth Annual Kansas State University Conference on Applied Statistics in Agriculture.* . 2008. Kansas State University
36. Champine, P.J., et al., *Microarray analysis reveals potential mechanisms of BRMS1-mediated metastasis suppression.* Clin Exp Metastasis, 2007. **24**(7): p. 551-65.

bioRxiv preprint doi: https://doi.org/10.1101/795617; this version posted October 9, 2019. The copyright holder for this preprint (which was not certified by peer review) is the author/funder. All rights reserved. No reuse allowed without permission.

37. St-Pierre, C., et al., *Transcriptome sequencing of neonatal thymic epithelial cells.* Sci Rep, 2013. **3**: p. 1860.
38. Ghulmiyyah, L.M., et al., *The role of oxidative stress in the developmental origin of adult hypertension.* Am J Obstet Gynecol, 2011. **205**(2): p. 155 e7-11.
39. Chen, S., et al., *Heat shock protein B6 potently increases non-small cell lung cancer growth.* Mol Med Rep, 2014. **10**(2): p. 677-82.
40. Gharibi, B., et al., *Inhibition of Akt/mTOR attenuates age-related changes in mesenchymal stem cells.* Stem Cells, 2014. **32**(8): p. 2256-66.
41. Liu, P., et al., *Cell-cycle-regulated activation of Akt kinase by phosphorylation at its carboxyl terminus.* Nature, 2014. **508**(7497): p. 541-5.
42. Song, G., G. Ouyang, and S. Bao, *The activation of Akt/PKB signaling pathway and cell survival.* J Cell Mol Med, 2005. **9**(1): p. 59-71.
43. Xu, N., et al., *Akt: a double-edged sword in cell proliferation and genome stability.* J Oncol, 2012. **2012**: p. 951724.
44. Hannappel, E. and T. Huff, *The thymosins. Prothymosin alpha, parathymosin, and beta-thymosins: structure and function.* Vitam Horm, 2003. **66**: p. 257-96.
45. Okamoto, K. and F. Isohashi, *Purification and primary structure of a macromolecular-translocation inhibitor II of glucocorticoid-receptor binding to nuclei from rat liver. Inhibitor II is the 11.5-kDa Zn2+-binding protein (parathymosin).* Eur J Biochem, 2000. **267**(1): p. 155-62.
46. Plaisant, M., et al., *Inhibition of hedgehog signaling decreases proliferation and clonogenicity of human mesenchymal stem cells.* PLoS One, 2011. **6**(2): p. e16798.
47. Adolphe, C., et al., *Patched 1 and patched 2 redundancy has a key role in regulating epidermal differentiation.* J Invest Dermatol, 2014. **134**(7): p. 1981-90.
48. Kemp, K., et al., *Inflammatory cytokine induced regulation of superoxide dismutase 3 expression by human mesenchymal stem cells.* Stem Cell Rev, 2010. **6**(4): p. 548-59.
49. Kemp, K., et al., *Mesenchymal stem cell-secreted superoxide dismutase promotes cerebellar neuronal survival.* J Neurochem, 2010. **114**(6): p. 1569-80.
50. Kwon, M.J., et al., *Role of superoxide dismutase 3 in skin inflammation.* J Dermatol Sci, 2012. **67**(2): p. 81-7.
51. Bowler, R.P., et al., *Extracellular superoxide dismutase attenuates lipopolysaccharide-induced neutrophilic inflammation.* Am J Respir Cell Mol Biol, 2004. **31**(4): p. 432-9.
52. Kim, Y., et al., *Regulation of skin inflammation and angiogenesis by EC-SOD via HIF-1alpha and NF-kappaB pathways.* Free Radic Biol Med, 2011. **51**(11): p. 1985-95.
53. Manni, M.L., et al., *Extracellular superoxide dismutase in macrophages augments bacterial killing by promoting phagocytosis.* Am J Pathol, 2011. **178**(6): p. 2752-9.
54. Helledie, T., et al., *Heparan sulfate enhances the self-renewal and therapeutic potential of mesenchymal stem cells from human adult bone marrow.* Stem Cells Dev, 2012. **21**(11): p. 1897-910.
55. Shakhova, O. and L. Sommer, *Neural crest-derived stem cells*, in *StemBook*. 2008: Cambridge (MA).
56. Sivanathan, K.N., et al., *Interferon-gamma modification of mesenchymal stem cells: implications of autologous and allogeneic mesenchymal stem cell therapy in allotransplantation.* Stem Cell Rev, 2014. **10**(3): p. 351-75.
57. Bi, W., et al., *Sox9 is required for cartilage formation.* Nat Genet, 1999. **22**(1): p. 85-9.
58. Bell, D.M., et al., *SOX9 directly regulates the type-II collagen gene.* Nat Genet, 1997.

bioRxiv preprint doi: https://doi.org/10.1101/795617; this version posted October 9, 2019. The copyright holder for this preprint (which was not certified by peer review) is the author/funder. All rights reserved. No reuse allowed without permission.

16(2): p. 174-8.
59. Han, Y. and V. Lefebvre, *L-Sox5 and Sox6 drive expression of the aggrecan gene in cartilage by securing binding of Sox9 to a far-upstream enhancer.* Mol Cell Biol, 2008. **28**(16): p. 4999-5013.
60. Shin, J., et al., *Comparative analysis of fatty acid-binding protein 4 promoters: conservation of peroxisome proliferator-activated receptor binding sites.* J Anim Sci, 2009. **87**(12): p. 3923-34.
61. Shi, H., et al., *PPAR gamma Regulates Genes Involved in Triacylglycerol Synthesis and Secretion in Mammary Gland Epithelial Cells of Dairy Goats.* PPAR Res, 2013. **2013**: p. 310948.
62. Bakhtiarizadeh, M.R., M. Moradi-Shahrbabak, and E. Ebrahimie, *Underlying functional genomics of fat deposition in adipose tissue.* Gene, 2013. **521**(1): p. 122-8.
63. Bernlohr, D.A., et al., *Tissue specific expression of p422 protein, a putative lipid carrier, in mouse adipocytes.* Biochem Biophys Res Commun, 1985. **132**(2): p. 850-5.
64. Viguet-Carrin, S., P. Garnero, and P.D. Delmas, *The role of collagen in bone strength.* Osteoporos Int, 2006. **17**(3): p. 319-36.
65. de Bernard, B., et al., *Biochemical and immunohistochemical evidence that in cartilage an alkaline phosphatase is a Ca2+-binding glycoprotein.* J Cell Biol, 1986. **103**(4): p. 1615-23.
66. Tenenbaum, H.C. and J.N. Heersche, *Differentiation of osteoblasts and formation of mineralized bone in vitro.* Calcif Tissue Int, 1982. **34**(1): p. 76-9.
67. Choi, J.Y., et al., *Expression patterns of bone-related proteins during osteoblastic differentiation in MC3T3-E1 cells.* J Cell Biochem, 1996. **61**(4): p. 609-18.
68. Nagata, T., et al., *Biosynthesis of bone proteins [SPP-1 (secreted phosphoprotein-1, osteopontin), BSP (bone sialoprotein) and SPARC (osteonectin)] in association with mineralized-tissue formation by fetal-rat calvarial cells in culture.* Biochem J, 1991. **274 (Pt 2)**: p. 513-20.
69. Kim, S.J., et al., *Stanniocalcin-1 protects retinal ganglion cells by inhibiting apoptosis and oxidative damage.* PLoS One, 2013. **8**(5): p. e63749.
70. Block, G.J., et al., *Multipotent stromal cells are activated to reduce apoptosis in part by upregulation and secretion of stanniocalcin-1.* Stem Cells, 2009. **27**(3): p. 670-81.
71. Suh, K.S., et al., *CLIC4, an intracellular chloride channel protein, is a novel molecular target for cancer therapy.* J Investig Dermatol Symp Proc, 2005. **10**(2): p. 105-9.
72. Suh, K.S., et al., *CLIC4 mediates and is required for Ca2+-induced keratinocyte differentiation.* J Cell Sci, 2007. **120**(Pt 15): p. 2631-40.
73. Xiong, C.J., et al., *Macrophage migration inhibitory factor inhibits the migration of cartilage end plate-derived stem cells by reacting with CD74.* PLoS One, 2012. **7**(8): p. e43984.
74. Fischer-Valuck, B.W., et al., *Migratory response of mesenchymal stem cells to macrophage migration inhibitory factor and its antagonist as a function of colony-forming efficiency.* Biotechnol Lett, 2010. **32**(1): p. 19-27.
75. Veevers-Lowe, J., et al., *Mesenchymal stem cell migration is regulated by fibronectin through alpha5beta1-integrin-mediated activation of PDGFR-beta and potentiation of growth factor signals.* J Cell Sci, 2011. **124**(Pt 8): p. 1288-300.
76. Ip, J.E., et al., *Mesenchymal stem cells use integrin beta1 not CXC chemokine receptor 4 for myocardial migration and engraftment.* Mol Biol Cell, 2007. **18**(8): p. 2873-82.

bioRxiv preprint doi: https://doi.org/10.1101/795617; this version posted October 9, 2019. The copyright holder for this preprint (which was not certified by peer review) is the author/funder. All rights reserved. No reuse allowed without permission.

643 77. Salasznyk, R.M., et al., *ERK signaling pathways regulate the osteogenic differentiation*
644 *of human mesenchymal stem cells on collagen I and vitronectin.* Cell Commun Adhes,
645 2004. **11**(5-6): p. 137-53.
646 78. Bonnet, N., S.J. Conway, and S.L. Ferrari, *Regulation of beta catenin signaling and*
647 *parathyroid hormone anabolic effects in bone by the matricellular protein periostin.* Proc
648 Natl Acad Sci U S A, 2012. **109**(37): p. 15048-53.
649 79. Cho, Y.H., et al., *Enhancement of MSC adhesion and therapeutic efficiency in ischemic*
650 *heart using lentivirus delivery with periostin.* Biomaterials, 2012. **33**(5): p. 1376-85.
651 80. Ling, L., V. Nurcombe, and S.M. Cool, *Wnt signaling controls the fate of mesenchymal*
652 *stem cells.* Gene, 2009. **433**(1-2): p. 1-7.
653 81. Palumbo, S. and W.J. Li, *Osteoprotegerin enhances osteogenesis of human mesenchymal*
654 *stem cells.* Tissue Eng Part A, 2013. **19**(19-20): p. 2176-87.
655 82. Tierney, E.G., et al., *High levels of ephrinB2 over-expression increases the osteogenic*
656 *differentiation of human mesenchymal stem cells and promotes enhanced cell mediated*
657 *mineralisation in a polyethyleneimine-ephrinB2 gene-activated matrix.* J Control Release,
658 2013. **165**(3): p. 173-82.
659 83. Tsai, K.S., et al., *Type I collagen promotes proliferation and osteogenesis of human*
660 *mesenchymal stem cells via activation of ERK and Akt pathways.* J Biomed Mater Res A,
661 2010. **94**(3): p. 673-82.
662 84. Park, S.J., et al., *Interaction of mesenchymal stem cells with fibroblast-like synoviocytes*
663 *via cadherin-11 promotes angiogenesis by enhanced secretion of placental growth factor.*
664 J Immunol, 2014. **192**(7): p. 3003-10.
665 85. Sun, J., *Enteric bacteria and cancer stem cells.* Cancers (Basel), 2010. **3**(1): p. 285-97.
666 86. Yuan, Y., et al., *Marrow mesenchymal stromal cells reduce methicillin-resistant*
667 *Staphylococcus aureus infection in rat models.* Cytotherapy, 2014. **16**(1): p. 56-63.
668 87. Maiti, A. and W.A. Jiranek, *Inhibition of Methicillin-resistant Staphylococcus aureus-*
669 *induced cytokines mRNA production in human bone marrow derived mesenchymal stem*
670 *cells by 1,25-dihydroxyvitamin D3.* BMC Cell Biol, 2014. **15**: p. 11.
671 88. Owen, T.A., et al., *Progressive development of the rat osteoblast phenotype in vitro:*
672 *reciprocal relationships in expression of genes associated with osteoblast proliferation*
673 *and differentiation during formation of the bone extracellular matrix.* J Cell Physiol,
674 1990. **143**(3): p. 420-30.
675 89. Cowles, E.A., et al., *Mineralization and the expression of matrix proteins during in vivo*
676 *bone development.* Calcif Tissue Int, 1998. **62**(1): p. 74-82.
677 90. Wang, K.X. and D.T. Denhardt, *Osteopontin: role in immune regulation and stress*
678 *responses.* Cytokine Growth Factor Rev, 2008. **19**(5-6): p. 333-45.
679 91. Zou, C., et al., *Osteopontin promotes mesenchymal stem cell migration and lessens cell*
680 *stiffness via integrin beta1, FAK, and ERK pathways.* Cell Biochem Biophys, 2013.
681 **65**(3): p. 455-62.
682 92. Ashkar, S., et al., *Eta-1 (osteopontin): an early component of type-1 (cell-mediated)*
683 *immunity.* Science, 2000. **287**(5454): p. 860-4.
684 93. Akiyama, H., *Control of chondrogenesis by the transcription factor Sox9.* Mod
685 Rheumatol, 2008. **18**(3): p. 213-9.
686 94. Joyce, M.E., et al., *Transforming growth factor-beta and the initiation of chondrogenesis*
687 *and osteogenesis in the rat femur.* J Cell Biol, 1990. **110**(6): p. 2195-207.
688 95. Wan, M. and X. Cao, *BMP signaling in skeletal development.* Biochem Biophys Res

bioRxiv preprint doi: https://doi.org/10.1101/795617; this version posted October 9, 2019. The copyright holder for this preprint (which was not certified by peer review) is the author/funder. All rights reserved. No reuse allowed without permission.

Commun, 2005. **328**(3): p. 651-7.
96. Suomi, S., et al., *MicroRNAs regulate osteogenesis and chondrogenesis of mouse bone marrow stromal cells.* Gene Regul Syst Bio, 2008. **2**: p. 177-91.
97. Hoshino, K., et al., *Cutting edge: Toll-like receptor 4 (TLR4)-deficient mice are hyporesponsive to lipopolysaccharide: evidence for TLR4 as the Lps gene product.* J Immunol, 1999. **162**(7): p. 3749-52.
98. Raicevic, G., et al., *Inflammation and Toll-like receptor ligation differentially affect the osteogenic potential of human mesenchymal stromal cells depending on their tissue origin.* Tissue Eng Part A, 2012. **18**(13-14): p. 1410-8.
99. Cho, H.H., et al., *NF-kappaB activation stimulates osteogenic differentiation of mesenchymal stem cells derived from human adipose tissue by increasing TAZ expression.* J Cell Physiol, 2010. **223**(1): p. 168-77.
100. Kawai, T. and S. Akira, *Signaling to NF-kappaB by Toll-like receptors.* Trends Mol Med, 2007. **13**(11): p. 460-9.
101. Oeckinghaus, A. and S. Ghosh, *The NF-kappaB family of transcription factors and its regulation.* Cold Spring Harb Perspect Biol, 2009. **1**(4): p. a000034.
102. Guihard, P., et al., *Induction of osteogenesis in mesenchymal stem cells by activated monocytes/macrophages depends on oncostatin M signaling.* Stem Cells, 2012. **30**(4): p. 762-72.
103. Kawai, T., et al., *Unresponsiveness of MyD88-deficient mice to endotoxin.* Immunity, 1999. **11**(1): p. 115-22.
104. Gewirtz, A.T., et al., *Salmonella typhimurium induces epithelial IL-8 expression via Ca(2+)-mediated activation of the NF-kappaB pathway.* J Clin Invest, 2000. **105**(1): p. 79-92.
105. Eckmann, L., M.F. Kagnoff, and J. Fierer, *Epithelial cells secrete the chemokine interleukin-8 in response to bacterial entry.* Infect Immun, 1993. **61**(11): p. 4569-74.
106. Rougier, F., et al., *IL-6 and IL-8 production by human bone marrow stromal cells.* Cytokine, 1998. **10**(2): p. 93-7.
107. Hoffmann, E., et al., *Multiple control of interleukin-8 gene expression.* J Leukoc Biol, 2002. **72**(5): p. 847-55.
108. Sumanasinghe, R.D., et al., *Expression of proinflammatory cytokines by human mesenchymal stem cells in response to cyclic tensile strain.* J Cell Physiol, 2009. **219**(1): p. 77-83.
109. Fuller, K., J.M. Owens, and T.J. Chambers, *Macrophage inflammatory protein-1 alpha and IL-8 stimulate the motility but suppress the resorption of isolated rat osteoclasts.* J Immunol, 1995. **154**(11): p. 6065-72.
110. Pricola, K.L., et al., *Interleukin-6 maintains bone marrow-derived mesenchymal stem cell stemness by an ERK1/2-dependent mechanism.* J Cell Biochem, 2009. **108**(3): p. 577-88.
111. Cho, T.J., et al., *Expression and role of interleukin-6 in distraction osteogenesis.* Calcif Tissue Int, 2007. **80**(3): p. 192-200.
112. Zhu, W., et al., *Hypoxia and serum deprivation-induced apoptosis in mesenchymal stem cells.* Stem Cells, 2006. **24**(2): p. 416-25.
113. Kim, D.H., et al., *Epoxyeicosatrienoic acid agonist regulates human mesenchymal stem cell-derived adipocytes through activation of HO-1-pAKT signaling and a decrease in PPARgamma.* Stem Cells Dev, 2010. **19**(12): p. 1863-73.

bioRxiv preprint doi: https://doi.org/10.1101/795617; this version posted October 9, 2019. The copyright holder for this preprint (which was not certified by peer review) is the author/funder. All rights reserved. No reuse allowed without permission.

Figure Legends:

Figure 1: Microbial Association with human and goat ASCs (A-F). ASCs presented a uniform pattern of ***Salmonella enterica* ssp *enterica* serotype Typhimurium LT2 (ST)** infection, the total associated bacteria were invaded, gASC show significantly higher invasion compared to human cells (A). ASCs susceptibility to invasion was not exclusive to ST, association patterns were microbe specific; 35%, 12% *Salmonella enterica* ssp *enterica* serotype Typhimurium 14028, and 25%, 100% *Salmonella enterica* ssp *enterica* serotype Enteritidis (BCW_4673) were invaded in goat and human ASCs respectively (B). In gASCs, 35% *Salmonella enterica* ssp *enterica* serotype Newport (BCW_1378) and in hASCs, 7% of *Salmonella enterica* ssp *enterica* serotype Saint Paul (BCW_88) were invaded (B). Intracellular ST was observed by TEM two hours post MSC co-incubation (D-F), consistent with control non-treated hASCs (C), ST infected cells showed no signs of cellular toxicity (D-F). ST adherence to hASC was observed at various sites (E-F). **Expression of immunomodulatory factors in ASCs post-microbial association (G-H).** Quantitative PCR analysis of IL6, PTGS2, NFKB1, TGFB1, PPARG, SPP1, and IL8 expression in (G) goat and (H) human ASCs treated with ST or LPS. Data is presented as fold change (± SEM) in relative to expression levels in non-treated cells ("C") (fold change ~1, indicated by the dotted line). Statistical significance of $P < 0.05$ is denoted by an asterisk (*), and $P < 0.01$ denoted by two asterisks (**).

Figure 2: Downstream trends analysis of differentially expressed genes in hASCs post microbial challenge. The IPA regulation z-score algorithm was used to identify biological functions expected to increase or decrease based on the gene expression changes described in our dataset. Predictions base on p-value and z-score; positive z-score implies an increase in the predicted function, a negative z-score a decrease (z-score ≥ 2 or ≤ -2 represented by orange dotted lines). P-values ≤ 0.05 (red dots determined by Fischer's exact test), illustrate a significant

bioRxiv preprint doi: https://doi.org/10.1101/795617; this version posted October 9, 2019. The copyright holder for this preprint (which was not certified by peer review) is the author/funder. All rights reserved. No reuse allowed without permission.

association between a given biological function and genes differentially expressed in our dataset ($P \leq 0.05$).

Figure 3.1: Network displays interactions between genes regulating cell cycle, cellular assembly and organization that were differentially expressed in hASCs treated for sixty minutes with ST compared with untreated control. Upregulated genes are colored in shades of red, down regulated in shades of green ($P \leq 0.05$). IPA inserted Genes in white because they are connected to this network; dashed and solid lines denote indirect and direct relationships between molecules. The IPA molecule activity predictor assessed the activity of molecules strongly connected to this network; blue and orange colored molecules are predicted to have decreased and increased activity, respectively.

Figure 3.2: Up regulation of superoxide dismutase 3 (SOD3) in hASCs following microbial challenge. The IPA molecule activity predictor assessed the activity of molecules strongly connected to SOD3 (colored in shade or red); orange colored molecules are predicted to have an increased activity, based on the increased expression of SOD3 in our dataset. IPA inserted Genes colored in white because they are connected to this network; dashed and solid lines denote indirect and direct relationships between molecules.

Figure 4: Trilineage staining of human and goat ASCs. Alizarin Red S staining of osteogenic differentiation in ASCs post-microbial association (4.1). hASCs (A-D) were cultured in osteogenic differentiation medium for 14 days, whereas gASCs (E-H) for 21 days and stained with Alizarin Red S. ASCs cultured in osteoinductive medium stained positive for calcium, (A-B and E-F, respectively), but did not stain when cultured in control medium (C-D and G-H, respectively), regardless of ST treatment. Representative images are shown in phase contrast at 40X magnification (scale bars represent 500 μm). Figure 4.2. Alcian Blue staining of

bioRxiv preprint doi: https://doi.org/10.1101/795617; this version posted October 9, 2019. The copyright holder for this preprint (which was not certified by peer review) is the author/funder. All rights reserved. No reuse allowed without permission.

chondrogenic differentiation in ASCs post-microbial association. Human (A-D) and goat (E-H) ASCs were cultured in chondrogenic differentiation medium for 14 days, and subsequently stained with Alcian Blue. Cellular condensation, as well ridge and micromass formations that stain positive was observed in human and goat ASCs induced for chondrogenesis (A-B and E-F, respectively), independent of ST treatment. Some background staining was observed in ST-treated and non-treated cells cultured in control medium, but cells remained in monolayer (C-D and G-H, respectively). Representative images are shown in phase contrast at 40X magnification (scale bars represent 500 μm). Figure 4.3 Oil Red O staining of adipogenic differentiation in ASCs post-microbial association. hASCs (A-D) and gASCs (E-H) were cultured in adipogenic induction medium for 21 days, and stained with Oil Red O. Accumulation of cytoplasmic lipid droplets were observed in ASCs induced for adipogenesis (A-B and E-F, respectively), independent of ST treatment. ST-treated and non-treated ASCs cultured in control medium did not yield lipid-positive cells (C-D and G-H, respectively). Representative images are shown in bright field at 200X magnification (scale bars represent 100 μm).

Figure 5: ASC expression of trilineage differentiation markers. Figure 5.1 Expression of osteogenic markers in ASCs post-microbial association. Quantitative PCR analysis of COL1A1, ALPL and SPP1 gene expression in A) human and B) goat ASCs induced with osteogenic differentiation medium and/or treated with S.T. Figure 5.2 Expression of chondrogenic markers post-microbial association**.** Quantitative PCR analysis of SOX9 expression in A) human and B) goat ASCs induced with chondrogenic differentiation medium and/or treated with S.T. Figure 5.3 Expression of adipogenic markers in ASCs post-microbial association**.** Quantitative PCR analysis of PPARG and FABP4 expression in A) human and B) goat ASCs induced with adipogenic induction medium and/or treated with ST. Data is presented as fold change (± SEM)

bioRxiv preprint doi: https://doi.org/10.1101/795617; this version posted October 9, 2019. The copyright holder for this preprint (which was not certified by peer review) is the author/funder. All rights reserved. No reuse allowed without permission.

805 relative to expression levels in non-treated, non-induced cells (fold change ~1, indicated by the
806 dotted line). Statistical significance of $P < 0.05$ is denoted by an asterisk (*), and $P < 0.01$
807 denoted by two asterisks (**).

808 **Figure 6.1: Downstream trends analysis of differentially expressed genes in hASCs induced**
809 **towards osteogenesis post microbial challenge.** The IPA regulation z-score algorithm was used
810 to identify biological functions expected to increase or decrease based on the gene expression
811 changes observed in our dataset. Predictions base on p-value and z-score; positive z-score
812 implies an increase in the predicted function, a negative z-score a decrease (z-score ≥ 2 or ≤ -2
813 represented by orange dotted lines). P-values ≤ 0.05 (red dots determined by Fischer's exact test),
814 illustrate a significant association between a given biological function and genes differentially
815 expressed in our dataset ($P \leq 0.05$).

816 **Figure 6.2: Network displays interactions between genes involved in cell signaling,**
817 **migration and differentiation that were differentially expressed in hASCs induced towards**
818 **an osteogenic lineage following ST challenge.** Up-regulated genes are colored in shades of red,
819 down-regulated in shades of green. Genes in white were inserted by IPA because they are
820 connected to this network; dashed and solid lines denote indirect and direct relationships
821 between molecules. The IPA molecule activity predictor assessed the activity of molecules
822 strongly connected to this network; blue and orange colored molecules are predicted to have
823 decreased and increased activity, respectively.
824

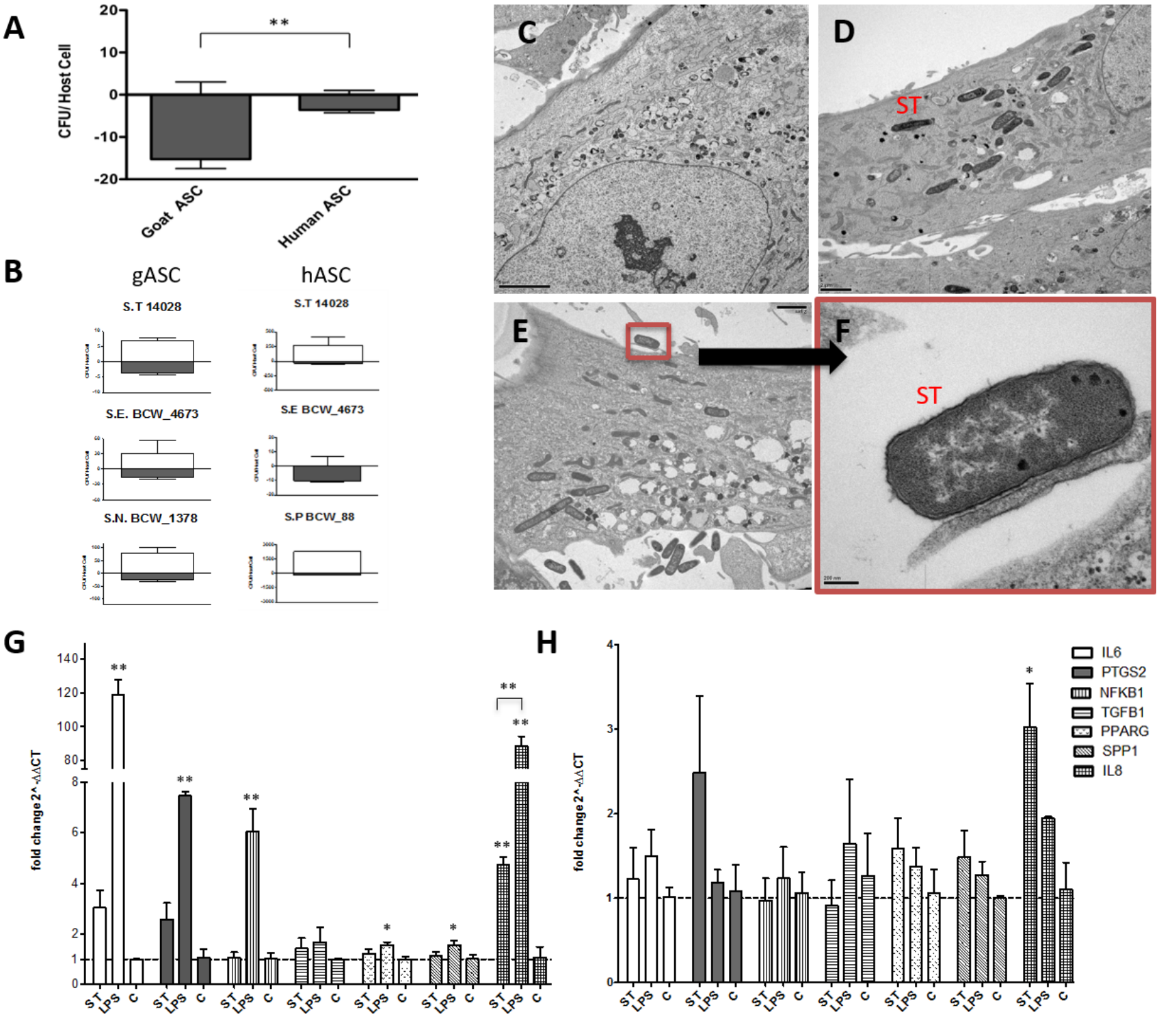
A
CFU/ Host Cell
20
10
0
-10
-20
**
Goat ASC
Human ASC
B
gASC
hASC
S.T 14028
S.T 14028
S.E. BCW_4673
S.E BCW_4673
S.N. BCW_1378
S.P BCW_88
C
D
ST
E
F
ST
G
fold change 2^-ΔΔCT
140
120
100
80
8
6
4
2
1
0
**
*
ST
LPS
C
H
fold change 2^-ΔΔCT
4
3
2
1
0
*
IL6
PTGS2
NFKB1
TGFB1
PPARG
SPP1
IL8

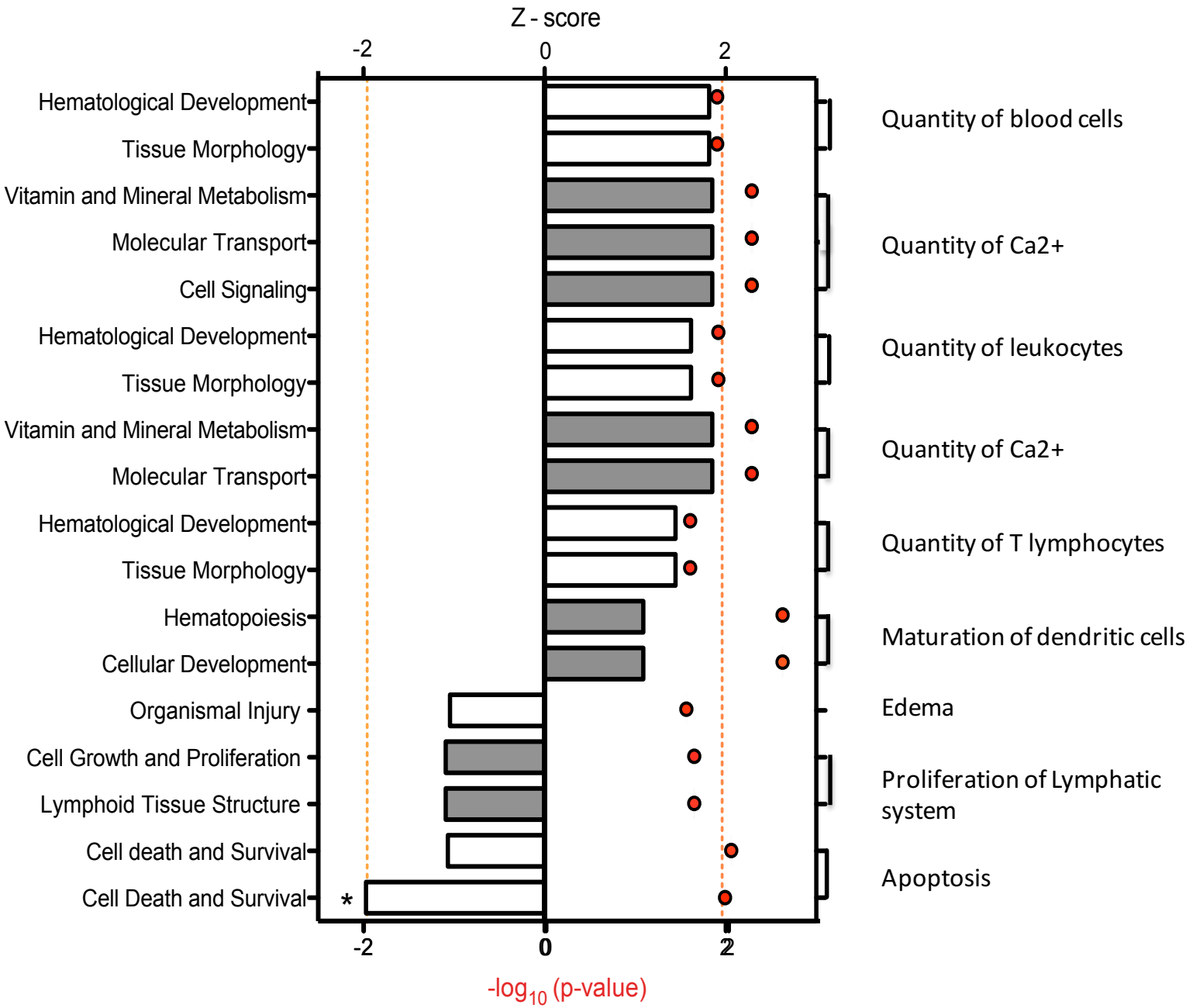
Z - score
-2
0
2
Hematological Development
Tissue Morphology
Vitamin and Mineral Metabolism
Molecular Transport
Cell Signaling
Hematological Development
Tissue Morphology
Vitamin and Mineral Metabolism
Molecular Transport
Hematological Development
Tissue Morphology
Hematopoiesis
Cellular Development
Organismal Injury
Cell Growth and Proliferation
Lymphoid Tissue Structure
Cell death and Survival
Cell Death and Survival
*
-2
0
2
-log10 (p-value)
Quantity of blood cells
Quantity of Ca2+
Quantity of leukocytes
Quantity of Ca2+
Quantity of T lymphocytes
Maturation of dendritic cells
Edema
Proliferation of Lymphatic system
Apoptosis

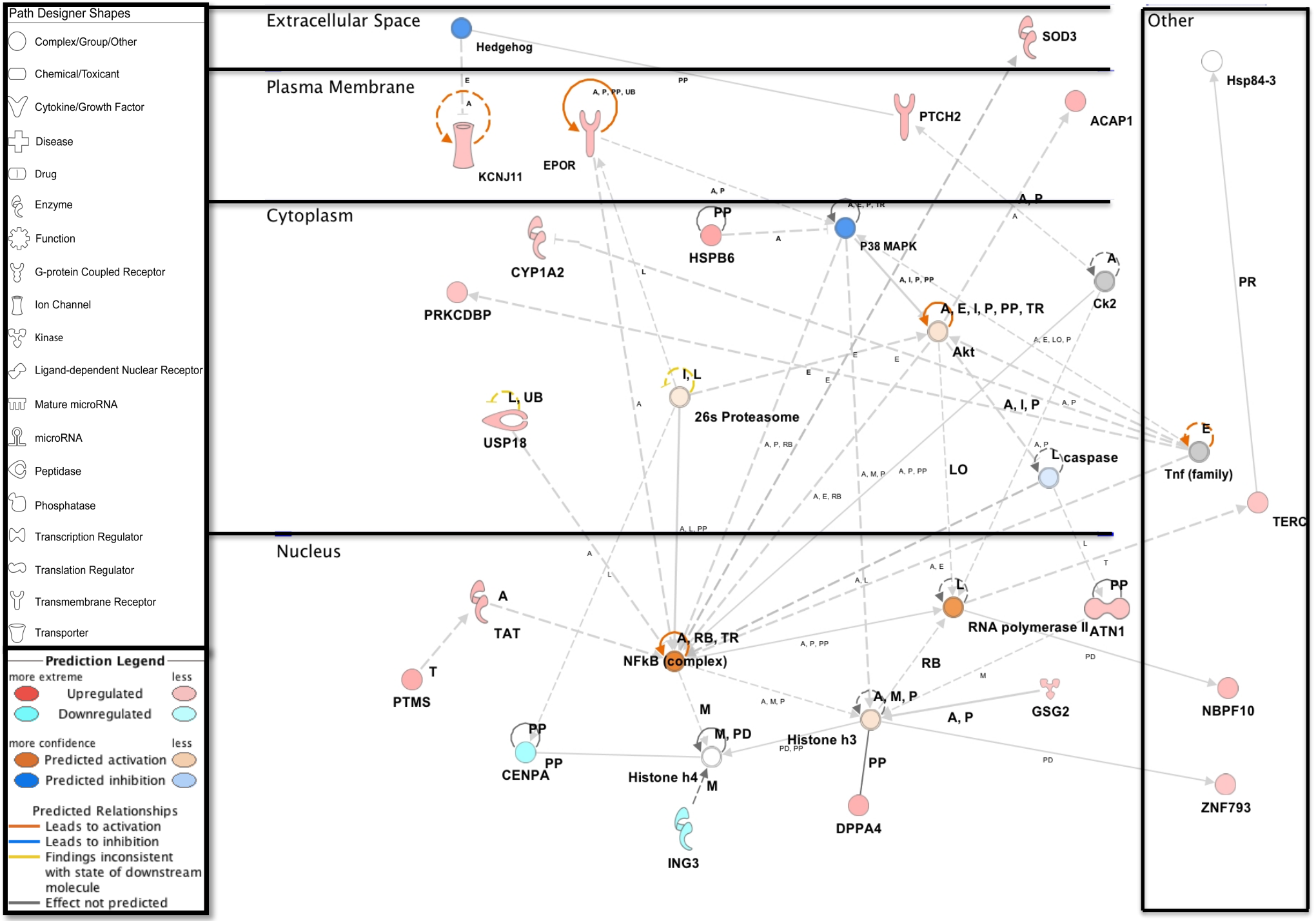
Path Designer Shapes
Complex/Group/Other
Chemical/Toxicant
Cytokine/Growth Factor
Disease
Drug
Enzyme
Function
G-protein Coupled Receptor
Ion Channel
Kinase
Ligand-dependent Nuclear Receptor
Mature microRNA
microRNA
Peptidase
Phosphatase
Transcription Regulator
Translation Regulator
Transmembrane Receptor
Transporter
Prediction Legend
more extreme
less
Upregulated
Downregulated
more confidence
less
Predicted activation
Predicted inhibition
Predicted Relationships
Leads to activation
Leads to inhibition
Findings inconsistent with state of downstream molecule
Effect not predicted
Extracellular Space
Plasma Membrane
Cytoplasm
Nucleus
Other
Hedgehog
SOD3
PTCH2
ACAP1
KCNJ11
EPOR
HSPB6
P38 MAPK
CYP1A2
PRKCDBP
Ck2
Akt
26s Proteasome
USP18
caspase
Tnf (family)
Hsp84-3
PR
TERC
TAT
PTMS
NFkB (complex)
RNA polymerase II
ATN1
NBPF10
GSG2
CENPA
Histone h4
Histone h3
DPPA4
ING3
ZNF793

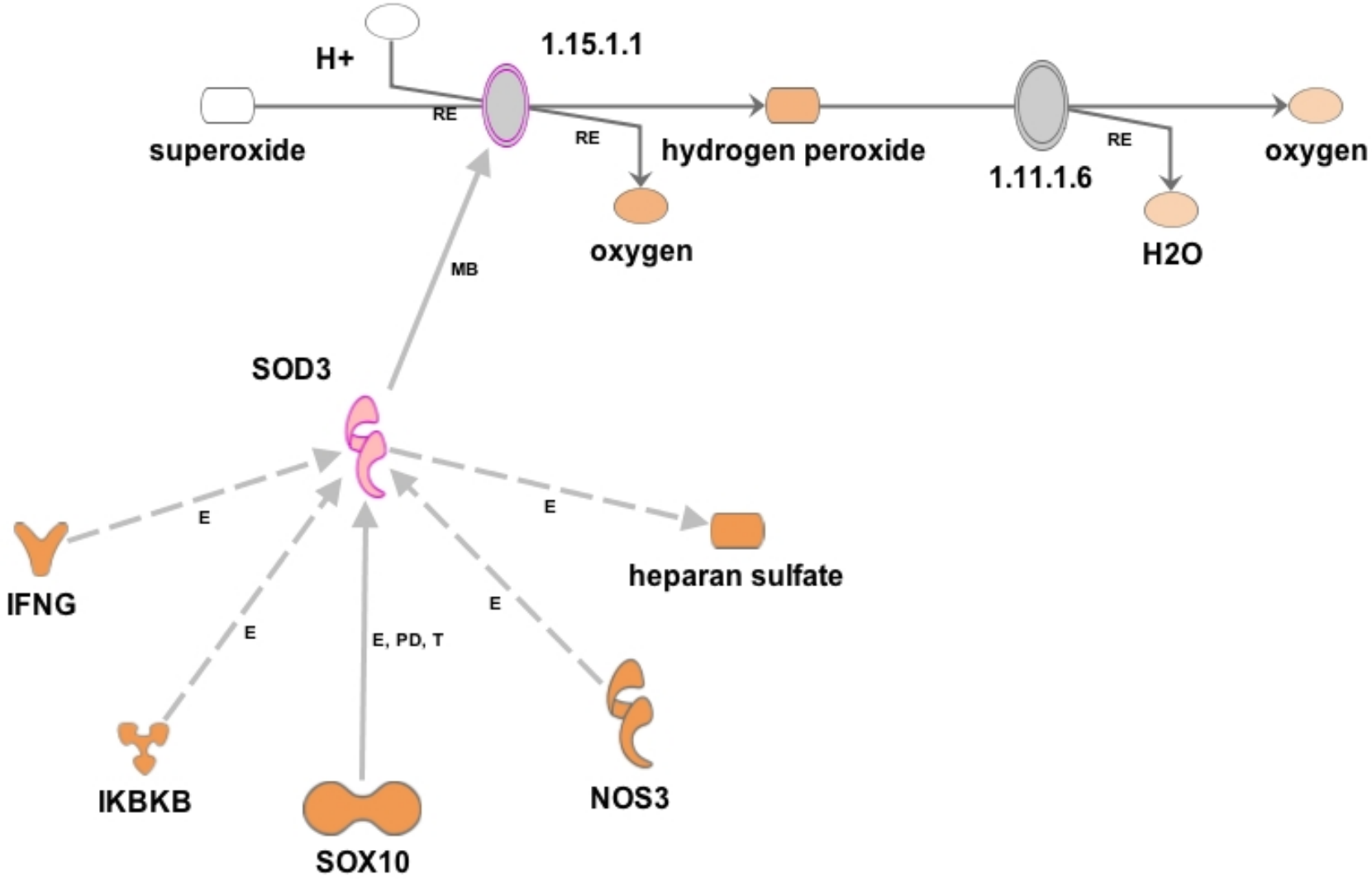
H+
1.15.1.1
RE
superoxide
RE
hydrogen peroxide
1.11.1.6
RE
oxygen
oxygen
H2O
MB
SOD3
E
IFNG
E
heparan sulfate
E
IKBKB
E, PD, T
SOX10
E
NOS3

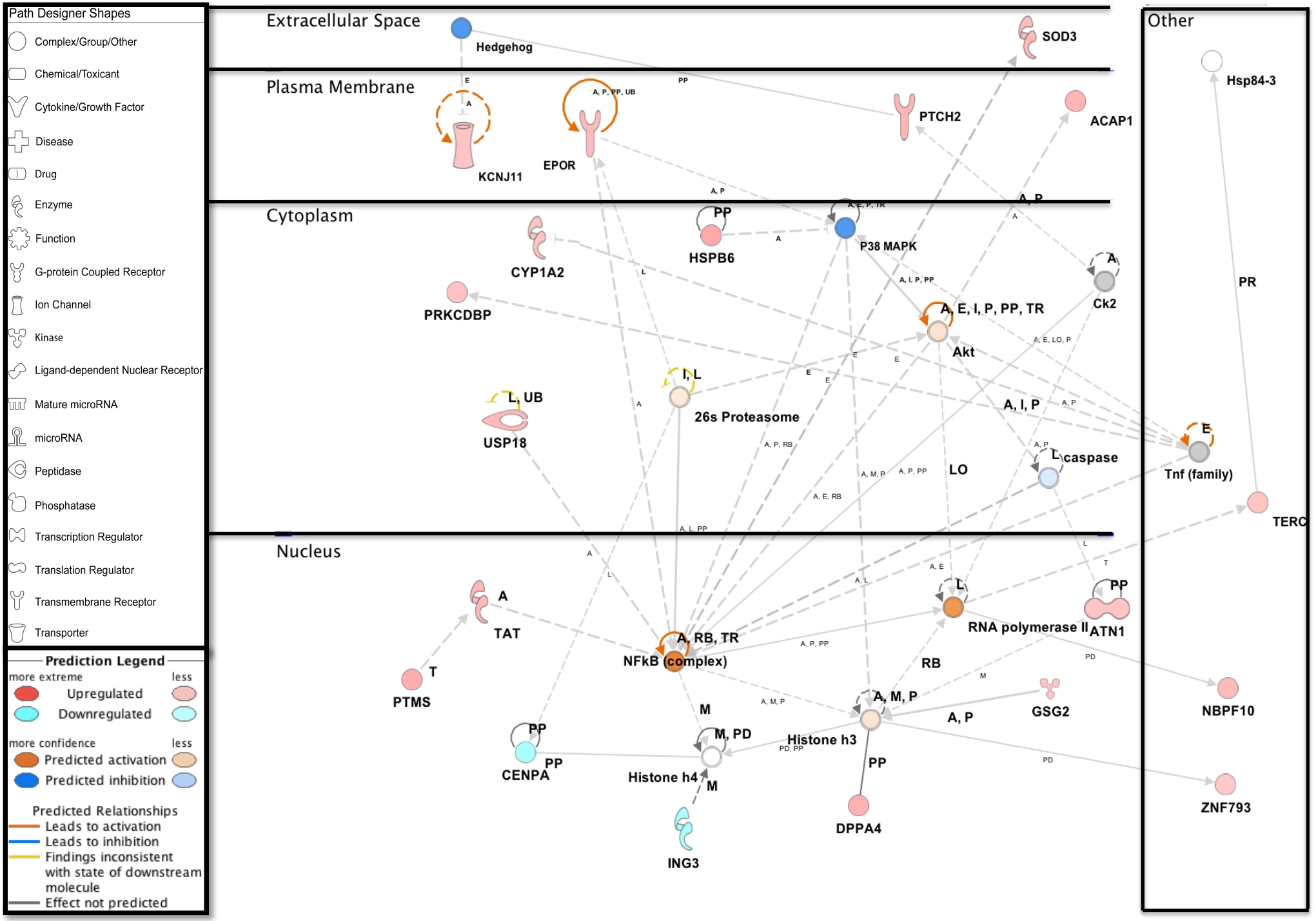
Path Designer Shapes
Complex/Group/Other
Chemical/Toxicant
Cytokine/Growth Factor
Disease
Drug
Enzyme
Function
G-protein Coupled Receptor
Ion Channel
Kinase
Ligand-dependent Nuclear Receptor
Mature microRNA
microRNA
Peptidase
Phosphatase
Transcription Regulator
Translation Regulator
Transmembrane Receptor
Transporter
Prediction Legend
more extreme
less
Upregulated
Downregulated
more confidence
less
Predicted activation
Predicted inhibition
Predicted Relationships
Leads to activation
Leads to inhibition
Findings inconsistent with state of downstream molecule
Effect not predicted
Extracellular Space
Plasma Membrane
Cytoplasm
Nucleus
Other
Hedgehog
SOD3
PTCH2
ACAP1
KCNJ11
EPOR
HSPB6
P38 MAPK
CYP1A2
PRKCDBP
Ck2
Akt
26s Proteasome
USP18
caspase
Tnf (family)
Hsp84-3
PR
TERC
TAT
PTMS
NFkB (complex)
RNA polymerase II
ATN1
NBPF10
GSG2
CENPA
Histone h4
Histone h3
DPPA4
ING3
ZNF793

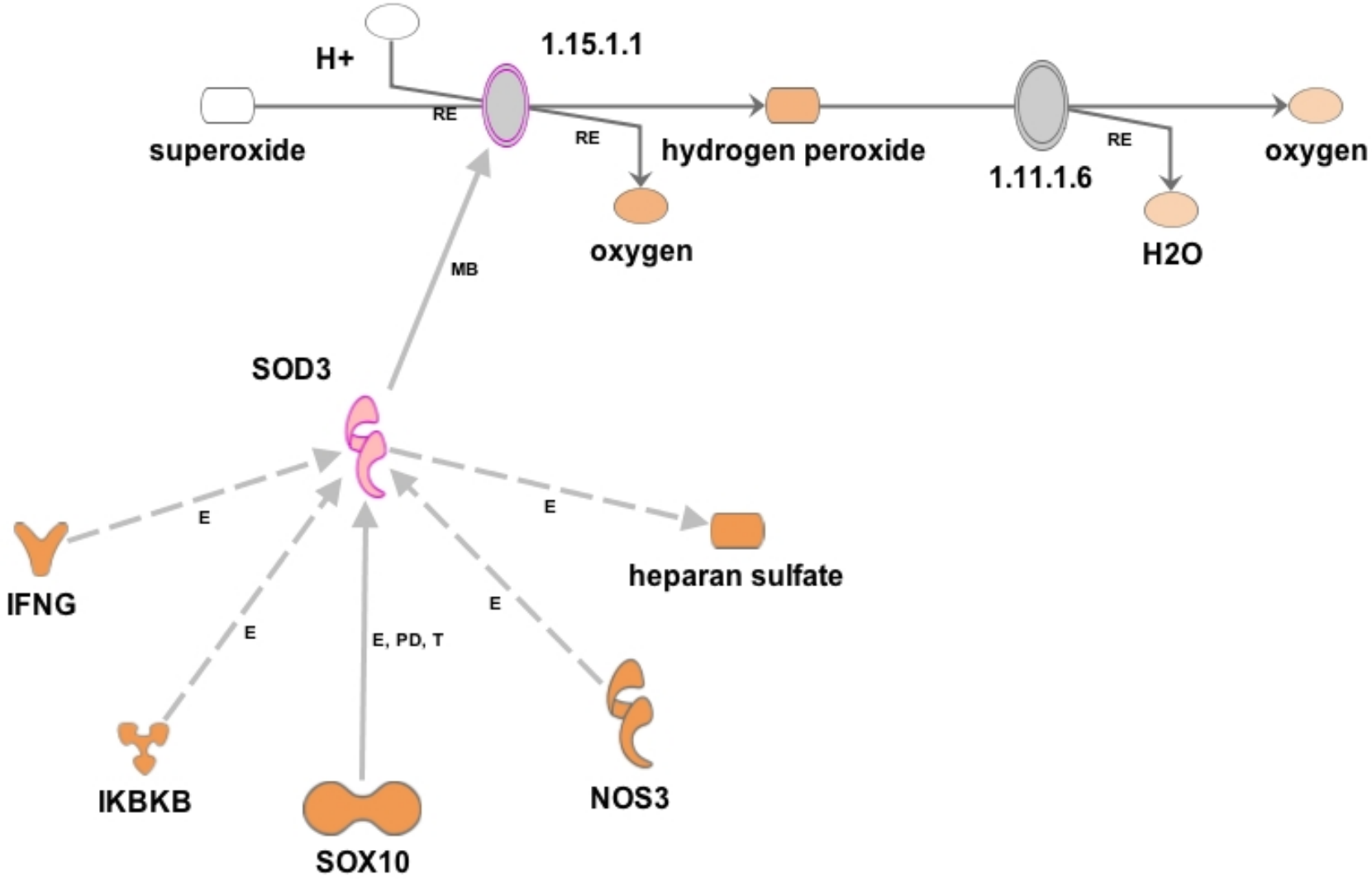
H+
1.15.1.1
RE
superoxide
RE
hydrogen peroxide
1.11.1.6
RE
oxygen
oxygen
H2O
MB
SOD3
E
IFNG
E
heparan sulfate
E
IKBKB
E, PD, T
SOX10
E
NOS3

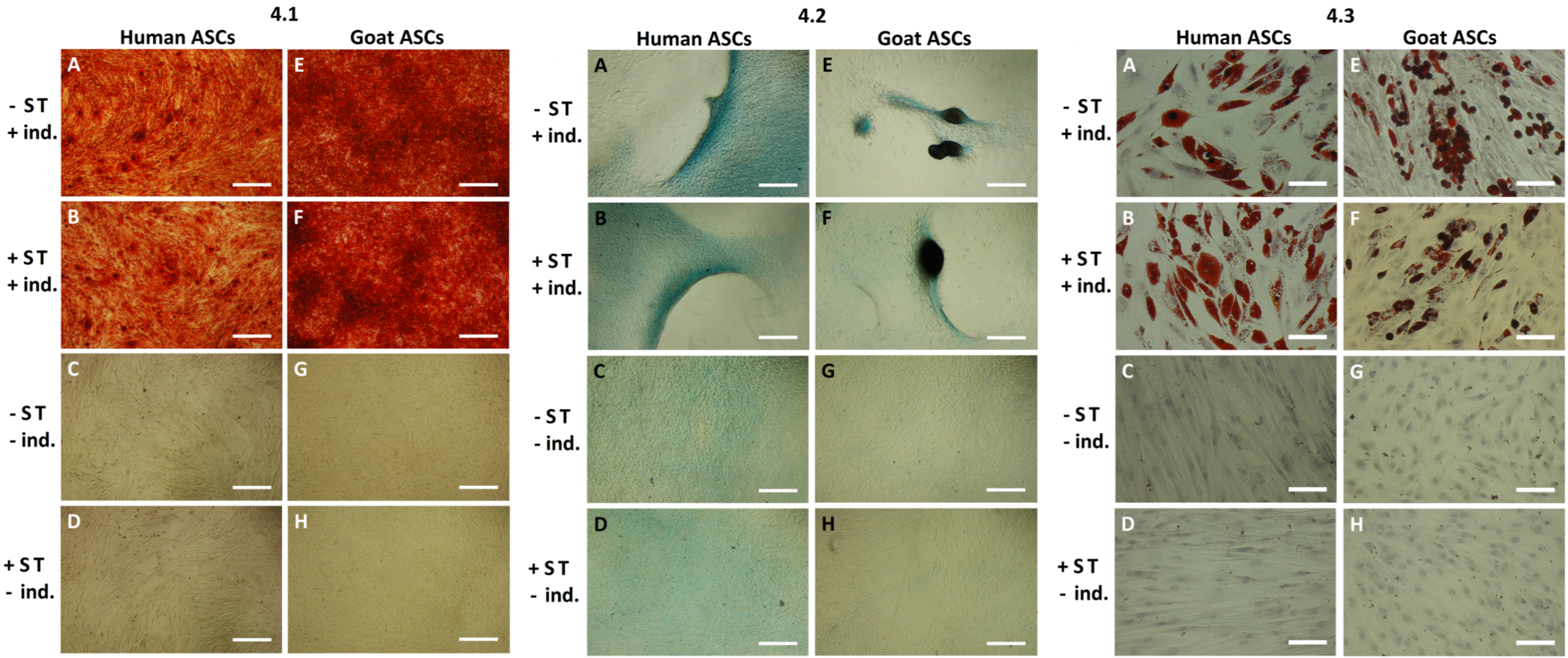
4.1
Human ASCs
Goat ASCs
A
E
- ST
+ ind.
B
F
+ ST
+ ind.
C
G
- ST
- ind.
D
H
+ ST
- ind.
4.2
Human ASCs
Goat ASCs
A
E
- ST
+ ind.
B
F
+ ST
+ ind.
C
G
- ST
- ind.
D
H
+ ST
- ind.
4.3
Human ASCs
Goat ASCs
A
E
- ST
+ ind.
B
F
+ ST
+ ind.
C
G
- ST
- ind.
D
H
+ ST
- ind.

5.1

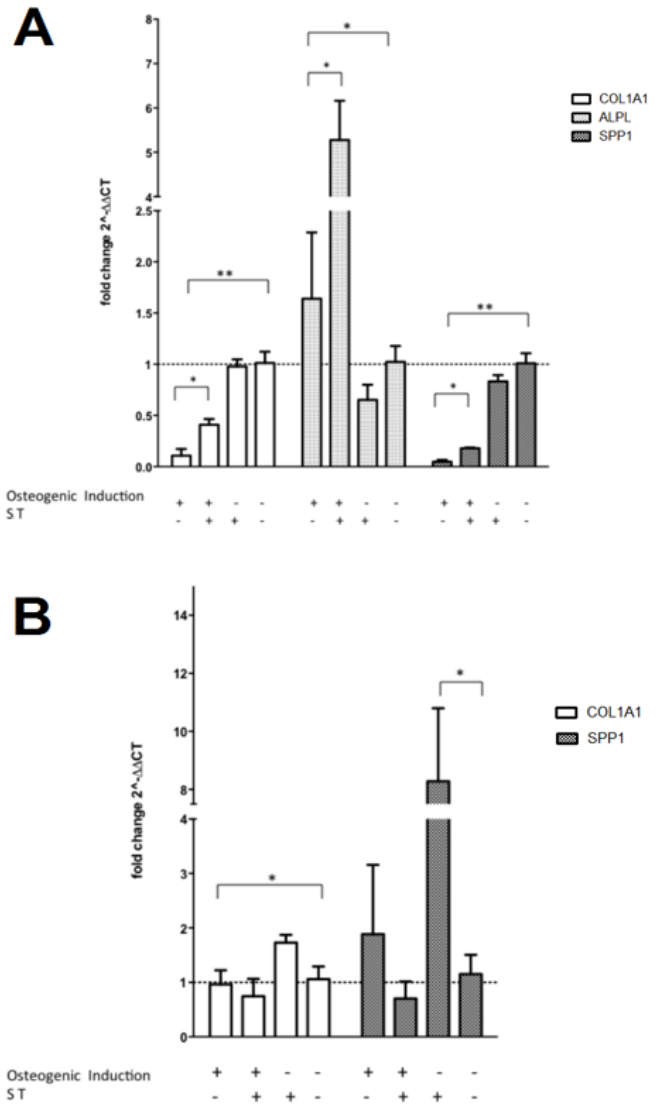
A
fold change 2^-ΔΔCT
COL1A1
ALPL
SPP1
Osteogenic Induction
ST
B
fold change 2^-ΔΔCT
COL1A1
SPP1
Osteogenic Induction
ST

5.2

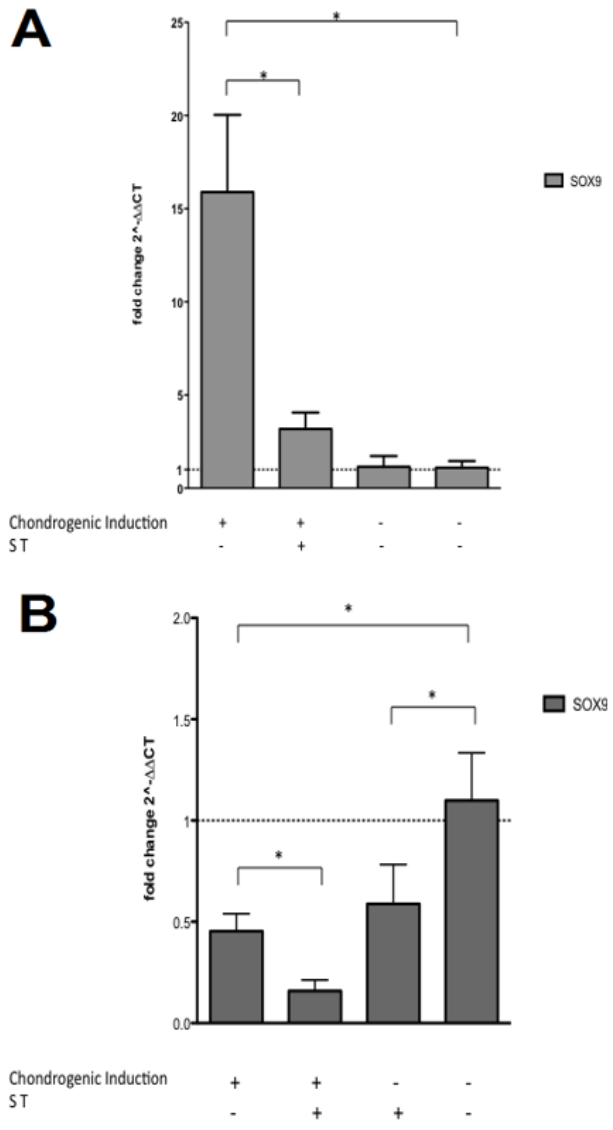
A
fold change 2^-ΔΔCT
SOX9
Chondrogenic Induction
ST
B
fold change 2^-ΔΔCT
SOX9
Chondrogenic Induction
ST

5.3

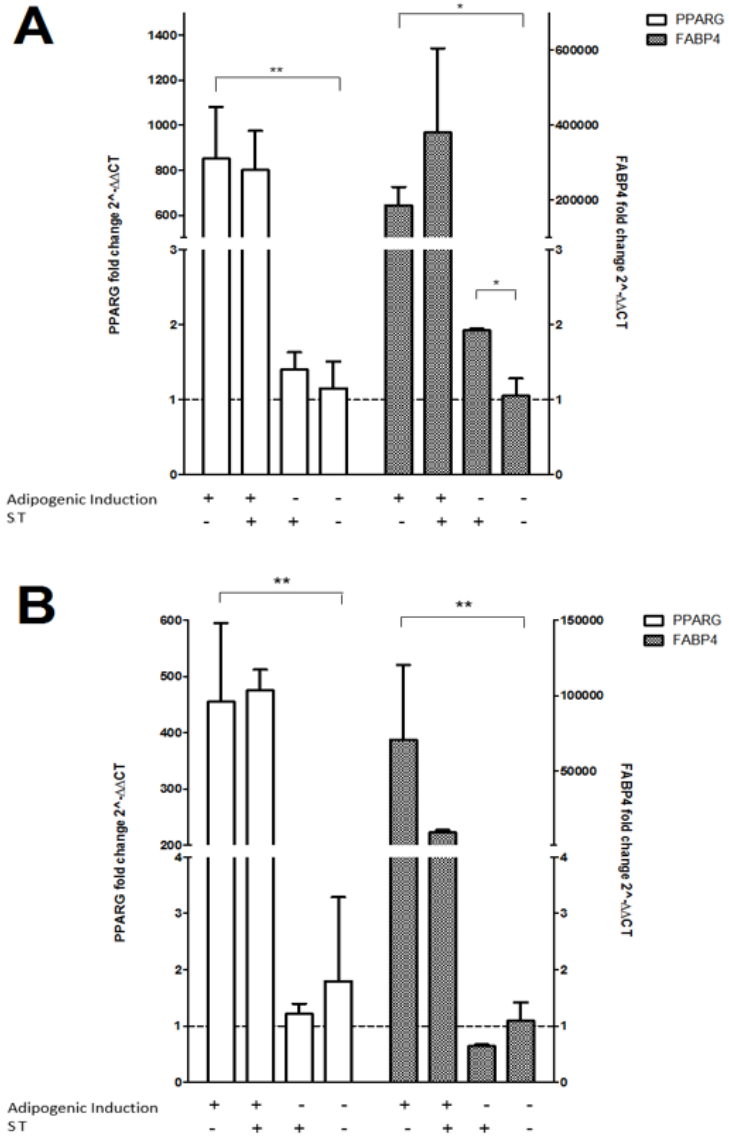
A
PPARG
FABP4
PPARG fold change 2^-ΔΔCT
FABP4 fold change 2^-ΔΔCT
Adipogenic Induction
ST
B
PPARG
FABP4
PPARG fold change 2^-ΔΔCT
FABP4 fold change 2^-ΔΔCT
Adipogenic Induction
ST

6.1

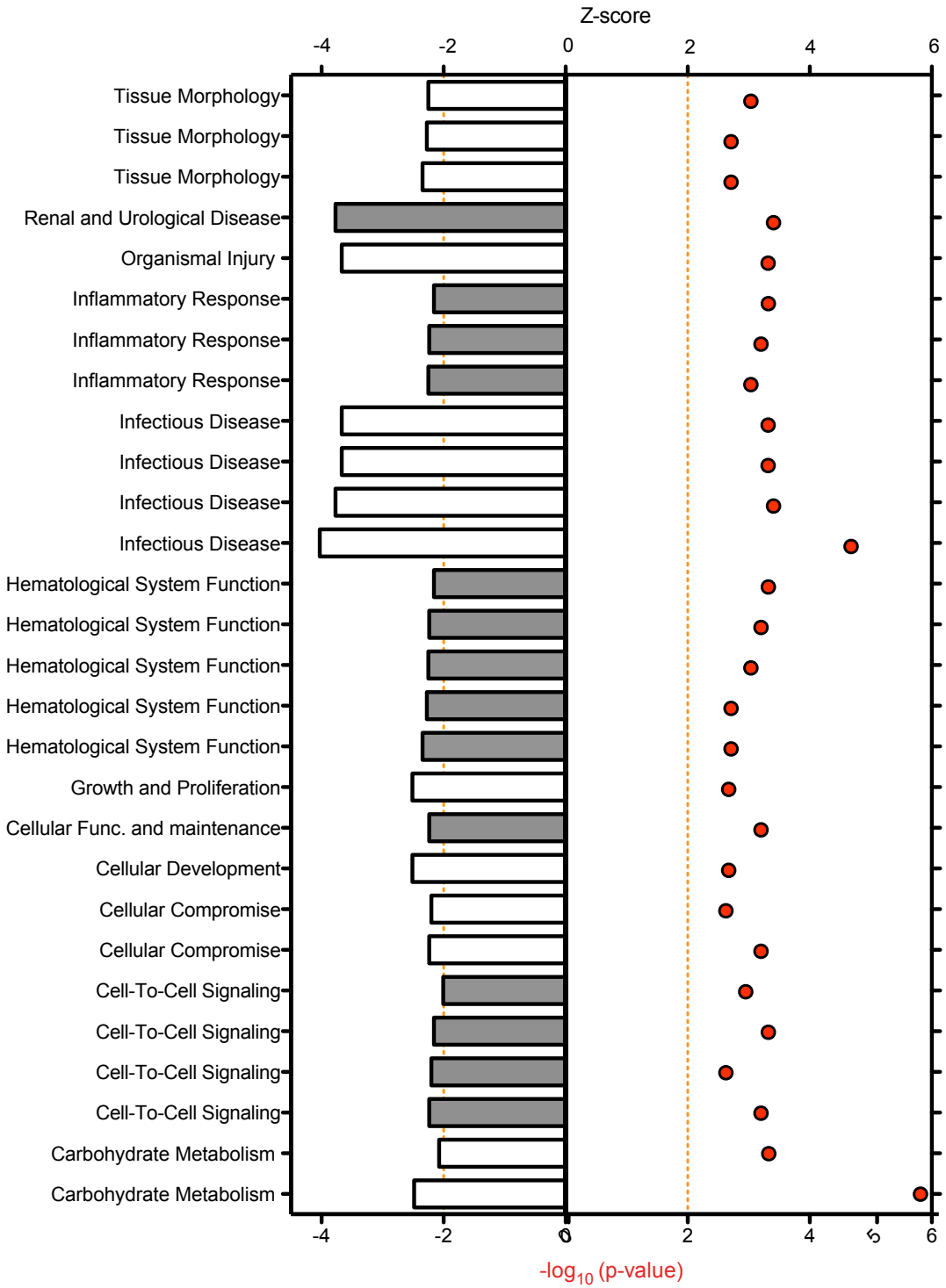
Z-score
-4
-2
0
2
4
6
Tissue Morphology
Tissue Morphology
Tissue Morphology
Renal and Urological Disease
Organismal Injury
Inflammatory Response
Inflammatory Response
Inflammatory Response
Infectious Disease
Infectious Disease
Infectious Disease
Infectious Disease
Hematological System Function
Hematological System Function
Hematological System Function
Hematological System Function
Hematological System Function
Growth and Proliferation
Cellular Func. and maintenance
Cellular Development
Cellular Compromise
Cellular Compromise
Cell-To-Cell Signaling
Cell-To-Cell Signaling
Cell-To-Cell Signaling
Cell-To-Cell Signaling
Carbohydrate Metabolism
Carbohydrate Metabolism
-4
-2
0
2
4
5
6
-log10 (p-value)

6.2

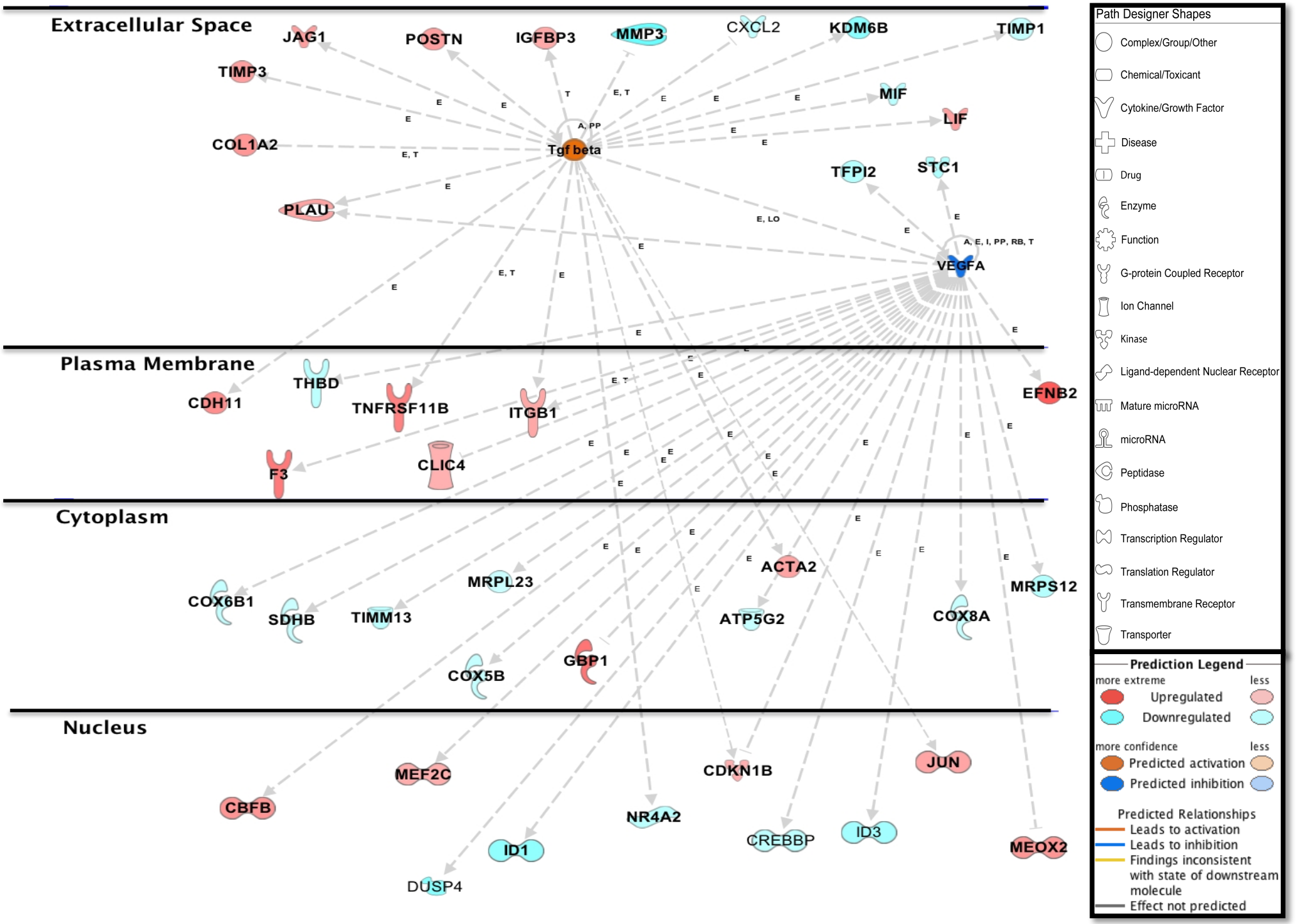
Extracellular Space
JAG1
POSTN
IGFBP3
MMP3
CXCL2
KDM6B
TIMP1
TIMP3
MIF
LIF
COL1A2
Tgf beta
TFPI2
STC1
PLAU
VEGFA
Plasma Membrane
THBD
CDH11
TNFRSF11B
ITGB1
EFNB2
F3
CLIC4
Cytoplasm
ACTA2
MRPL23
MRPS12
COX6B1
SDHB
TIMM13
ATP5G2
COX8A
COX5B
GBP1
Nucleus
MEF2C
CDKN1B
JUN
CBFB
NR4A2
CREBBP
ID3
ID1
MEOX2
DUSP4
Path Designer Shapes
Complex/Group/Other
Chemical/Toxicant
Cytokine/Growth Factor
Disease
Drug
Enzyme
Function
G-protein Coupled Receptor
Ion Channel
Kinase
Ligand-dependent Nuclear Receptor
Mature microRNA
microRNA
Peptidase
Phosphatase
Transcription Regulator
Translation Regulator
Transmembrane Receptor
Transporter
Prediction Legend
more extreme
less
Upregulated
Downregulated
more confidence
less
Predicted activation
Predicted inhibition
Predicted Relationships
Leads to activation
Leads to inhibition
Findings inconsistent with state of downstream molecule
Effect not predicted